

Singapore Management University

Institutional Knowledge at Singapore Management University

Research Collection School Of Computing and Information Systems

School of Computing and Information Systems

1-1998

Search for supersymmetry with a dominant R-parity violating $LL\bar{E}$ coupling in e^+e^- collisions at centre-of-mass energies of 130 GeV to 172 GeV

R. BARATE

M. THULASIDAS

Singapore Management University, manojt@smu.edu.sg

Follow this and additional works at: https://ink.library.smu.edu.sg/sis_research



Part of the [Databases and Information Systems Commons](#)

Citation

1

This Journal Article is brought to you for free and open access by the School of Computing and Information Systems at Institutional Knowledge at Singapore Management University. It has been accepted for inclusion in Research Collection School Of Computing and Information Systems by an authorized administrator of Institutional Knowledge at Singapore Management University. For more information, please email cherylds@smu.edu.sg.

Search for Supersymmetry with a dominant R-Parity
violating $LL\bar{E}$ Coupling in e^+e^- Collisions
at centre-of-mass energies of 130 GeV to 172 GeV

The ALEPH Collaboration^{*)}

Abstract

A search for pair-production of supersymmetric particles under the assumption that R-parity is violated via a dominant $LL\bar{E}$ coupling has been performed using the data collected by ALEPH at centre-of-mass energies of 130–172 GeV. The observed candidate events in the data are in agreement with the Standard Model expectation. This is translated into lower limits on the mass of charginos, neutralinos, sleptons, sneutrinos and squarks. For instance, charginos with masses less than $73 \text{ GeV}/c^2$ and neutralinos with masses less than $23 \text{ GeV}/c^2$ are excluded at 95% confidence level for any generation structure of the $LL\bar{E}$ coupling, and for neutralino, slepton or sneutrino LSPs.

Submitted to Zeitschrift für Physik C

^{*)} See next pages for the list of authors

The ALEPH Collaboration

R. Barate, D. Buskalic, D. Decamp, P. Ghez, C. Goy, J.-P. Lees, A. Lucotte, M.-N. Minard, J.-Y. Nief, B. Pietrzyk

Laboratoire de Physique des Particules (LAPP), IN²P³-CNRS, 74019 Annecy-le-Vieux Cedex, France

G. Boix, M.P. Casado, M. Chmeissani, J.M. Crespo, M. Delfino, E. Fernandez, M. Fernandez-Bosman, Ll. Garrido,¹⁵ E. Graugès, A. Juste, M. Martinez, G. Merino, R. Miquel, Ll.M. Mir, P. Morawitz, I.C. Park, A. Pascual, J.A. Perlas, I. Riu, F. Sanchez

Institut de Física d'Altes Energies, Universitat Autònoma de Barcelona, 08193 Bellaterra (Barcelona), Spain⁷

A. Colaleo, D. Creanza, M. de Palma, G. Gelao, G. Iaselli, G. Maggi, M. Maggi, N. Marinelli, S. Nuzzo, A. Ranieri, G. Raso, F. Ruggieri, G. Selvaggi, L. Silvestris, P. Tempesta, A. Tricomi,³ G. Zito

Dipartimento di Fisica, INFN Sezione di Bari, 70126 Bari, Italy

X. Huang, J. Lin, Q. Ouyang, T. Wang, Y. Xie, R. Xu, S. Xue, J. Zhang, L. Zhang, W. Zhao

Institute of High-Energy Physics, Academia Sinica, Beijing, The People's Republic of China⁸

D. Abbaneo, R. Alemany, U. Becker, P. Bright-Thomas, D. Casper, M. Cattaneo, F. Cerutti, V. Ciulli, G. Dissertori, H. Drevermann, R.W. Forty, M. Frank, F. Gianotti, R. Hagelberg, J.B. Hansen, J. Harvey, P. Janot, B. Jost, I. Lehraus, P. Mato, A. Minten, L. Moneta, A. Pacheco, J.-F. Puztaszeri,²⁰ F. Ranjard, L. Rolandi, D. Rousseau, D. Schlatter, M. Schmitt, O. Schneider, W. Tejessy, F. Teubert, I.R. Tomalin, M. Vreeswijk, H. Wachsmuth, A. Wagner¹

European Laboratory for Particle Physics (CERN), 1211 Geneva 23, Switzerland

Z. Ajaltouni, F. Badaud, G. Chazelle, O. Deschamps, A. Falvard, C. Ferdi, P. Gay, C. Guicheney, P. Henrard, J. Jousset, B. Michel, S. Monteil, J.-C. Montret, D. Pallin, P. Perret, F. Podlyski, J. Proriot, P. Rosnet

Laboratoire de Physique Corpusculaire, Université Blaise Pascal, IN²P³-CNRS, Clermont-Ferrand, 63177 Aubière, France

T. Fearnley, J.D. Hansen, J.R. Hansen, P.H. Hansen, B.S. Nilsson, B. Rensch, A. Wäänänen

Niels Bohr Institute, 2100 Copenhagen, Denmark⁹

G. Daskalakis, A. Kyriakis, C. Markou, E. Simopoulou, A. Vayaki

Nuclear Research Center Demokritos (NRCD), Athens, Greece

A. Blondel, J.-C. Brient, F. Machefert, A. Rougé, M. Rumpf, A. Valassi,⁶ H. Videau

Laboratoire de Physique Nucléaire et des Hautes Energies, Ecole Polytechnique, IN²P³-CNRS, 91128 Palaiseau Cedex, France

T. Boccali, E. Focardi, G. Parrini, K. Zachariadou

Dipartimento di Fisica, Università di Firenze, INFN Sezione di Firenze, 50125 Firenze, Italy

R. Cavanaugh, M. Corden, C. Georgiopoulos, T. Huehn, D.E. Jaffe

Supercomputer Computations Research Institute, Florida State University, Tallahassee, FL 32306-4052, USA^{13,14}

A. Antonelli, G. Bencivenni, G. Bologna,⁴ F. Bossi, P. Campana, G. Capon, V. Chiarella, G. Felici, P. Laurelli, G. Mannocchi,⁵ F. Murtas, G.P. Murtas, L. Passalacqua, M. Pepe-Altarelli

Laboratori Nazionali dell'INFN (LNF-INFN), 00044 Frascati, Italy

L. Curtis, S.J. Dorris, A.W. Halley, J.G. Lynch, P. Negus, V. O'Shea, C. Raine, J.M. Scarr, K. Smith,

- P. Teixeira-Dias, A.S. Thompson, E. Thomson, F. Thomson
*Department of Physics and Astronomy, University of Glasgow, Glasgow G12 8QQ, United Kingdom*¹⁰
- O. Buchmüller, S. Dhamotharan, C. Geweniger, G. Graefe, P. Hanke, G. Hansper, V. Hepp, E.E. Kluge, A. Putzer, J. Sommer, K. Tittel, S. Werner, M. Wunsch
*Institut für Hochenergiephysik, Universität Heidelberg, 69120 Heidelberg, Fed. Rep. of Germany*¹⁶
- R. Beuselinck, D.M. Binnie, W. Cameron, P.J. Dornan, M. Girone, S. Goodsir, E.B. Martin, A. Moutoussi, J. Nash, J.K. Sedgbeer, P. Spagnolo, M.D. Williams
*Department of Physics, Imperial College, London SW7 2BZ, United Kingdom*¹⁰
- V.M. Ghete, P. Girtler, E. Kneringer, D. Kuhn, G. Rudolph
*Institut für Experimentalphysik, Universität Innsbruck, 6020 Innsbruck, Austria*¹⁸
- A.P. Betteridge, C.K. Bowdery, P.G. Buck, P. Colrain, G. Crawford, A.J. Finch, F. Foster, G. Hughes, R.W.L. Jones, E.P. Whelan, M.I. Williams
*Department of Physics, University of Lancaster, Lancaster LA1 4YB, United Kingdom*¹⁰
- I. Giehl, C. Hoffmann, K. Jakobs, K. Kleinknecht, G. Quast, B. Renk, E. Rohne, H.-G. Sander, P. van Gemmeren, C. Zeitnitz
*Institut für Physik, Universität Mainz, 55099 Mainz, Fed. Rep. of Germany*¹⁶
- J.J. Aubert, C. Benchouk, A. Bonissent, G. Bujosa, J. Carr, P. Coyle, C. Diaconu, A. Ealet, D. Fouchez, O. Leroy, F. Motsch, P. Payre, M. Talby, A. Sadouki, M. Thulasidas, A. Tilquin, K. Trabelsi
Centre de Physique des Particules, Faculté des Sciences de Luminy, IN²P³-CNRS, 13288 Marseille, France
- M. Aleppo, M. Antonelli, F. Ragusa
Dipartimento di Fisica, Università di Milano e INFN Sezione di Milano, 20133 Milano, Italy.
- R. Berlich, W. Blum, V. Büscher, H. Dietl, G. Ganis, C. Gotzhein, H. Kroha, G. Lütjens, G. Lutz, C. Mannert, W. Männer, H.-G. Moser, R. Richter, A. Rosado-Schlosser, S. Schael, R. Settles, H. Seywerd, H. Stenzel, W. Wiedenmann, G. Wolf
*Max-Planck-Institut für Physik, Werner-Heisenberg-Institut, 80805 München, Fed. Rep. of Germany*¹⁶
- J. Boucrot, O. Callot,¹² S. Chen, M. Davier, L. Duflot, J.-F. Grivaz, Ph. Heusse, A. Höcker, A. Jacholkowska, M.M. Kado, D.W. Kim,² F. Le Diberder, J. Lefrançois, A.-M. Lutz, M.-H. Schune, L. Serin, E. Tournefier, J.-J. Veillet, I. Videau, D. Zerwas
Laboratoire de l'Accélérateur Linéaire, Université de Paris-Sud, IN²P³-CNRS, 91405 Orsay Cedex, France
- P. Azzurri, G. Bagliesi,¹² S. Bettarini, C. Bozzi, G. Calderini, R. Dell'Orso, R. Fantechi, I. Ferrante, A. Giassi, A. Gregorio, F. Ligabue, A. Lusiani, P.S. Marrocchesi, A. Messineo, F. Palla, G. Rizzo, G. Sanguinetti, A. Sciabà, G. Sguazzoni, J. Steinberger, R. Tenchini, C. Vannini, A. Venturi, P.G. Verdini
Dipartimento di Fisica dell'Università, INFN Sezione di Pisa, e Scuola Normale Superiore, 56010 Pisa, Italy
- G.A. Blair, L.M. Bryant, J.T. Chambers, J. Coles, M.G. Green, T. Medcalf, P. Perrodo, J.A. Strong, J.H. von Wimmersperg-Toeller
*Department of Physics, Royal Holloway & Bedford New College, University of London, Surrey TW20 OEX, United Kingdom*¹⁰
- D.R. Botterill, R.W. Clift, T.R. Edgecock, S. Haywood, P. Maley, P.R. Norton, J.C. Thompson, A.E. Wright
*Particle Physics Dept., Rutherford Appleton Laboratory, Chilton, Didcot, Oxon OX11 0QX, United Kingdom*¹⁰

B. Bloch-Devaux, P. Colas, B. Fabbro, G. Faïf, E. Lançon, M.-C. Lemaire, E. Locci, P. Perez, H. Przysiezniak, J. Rander, J.-F. Renardy, A. Rosowsky, A. Roussarie, A. Trabelsi, B. Vallage

*CEA, DAPNIA/Service de Physique des Particules, CE-Saclay, 91191 Gif-sur-Yvette Cedex, France*¹⁷

S.N. Black, J.H. Dann, H.Y. Kim, N. Konstantinidis, A.M. Litke, M.A. McNeil, G. Taylor

*Institute for Particle Physics, University of California at Santa Cruz, Santa Cruz, CA 95064, USA*¹⁹

C.N. Booth, C.A.J. Brew, S. Cartwright, F. Combley, M.S. Kelly, M. Lehto, J. Reeve, L.F. Thompson

*Department of Physics, University of Sheffield, Sheffield S3 7RH, United Kingdom*¹⁰

K. Affholderbach, A. Böhrer, S. Brandt, G. Cowan, J. Foss, C. Grupen, L. Smolik, F. Stephan

*Fachbereich Physik, Universität Siegen, 57068 Siegen, Fed. Rep. of Germany*¹⁶

M. Apollonio, L. Bosisio, R. Della Marina, G. Giannini, B. Gobbo, G. Musolino

Dipartimento di Fisica, Università di Trieste e INFN Sezione di Trieste, 34127 Trieste, Italy

J. Putz, J. Rothberg, S. Wasserbaech, R.W. Williams

Experimental Elementary Particle Physics, University of Washington, WA 98195 Seattle, U.S.A.

S.R. Armstrong, E. Charles, P. Elmer, D.P.S. Ferguson, Y. Gao, S. González, T.C. Greening, O.J. Hayes, H. Hu, S. Jin, P.A. McNamara III, J.M. Nachtman,²¹ J. Nielsen, W. Orejudos, Y.B. Pan, Y. Saadi, I.J. Scott, J. Walsh, Sau Lan Wu, X. Wu, J.M. Yamartino, G. Zoernig

*Department of Physics, University of Wisconsin, Madison, WI 53706, USA*¹¹

¹Now at Schweizerischer Bankverein, Basel, Switzerland.

²Permanent address: Kangnung National University, Kangnung, Korea.

³Also at Dipartimento di Fisica, INFN Sezione di Catania, Catania, Italy.

⁴Also Istituto di Fisica Generale, Università di Torino, Torino, Italy.

⁵Also Istituto di Cosmo-Geofisica del C.N.R., Torino, Italy.

⁶Supported by the Commission of the European Communities, contract ERBCHBICT941234.

⁷Supported by CICYT, Spain.

⁸Supported by the National Science Foundation of China.

⁹Supported by the Danish Natural Science Research Council.

¹⁰Supported by the UK Particle Physics and Astronomy Research Council.

¹¹Supported by the US Department of Energy, grant DE-FG0295-ER40896.

¹²Also at CERN, 1211 Geneva 23, Switzerland.

¹³Supported by the US Department of Energy, contract DE-FG05-92ER40742.

¹⁴Supported by the US Department of Energy, contract DE-FC05-85ER250000.

¹⁵Permanent address: Universitat de Barcelona, 08208 Barcelona, Spain.

¹⁶Supported by the Bundesministerium für Bildung, Wissenschaft, Forschung und Technologie, Fed. Rep. of Germany.

¹⁷Supported by the Direction des Sciences de la Matière, C.E.A.

¹⁸Supported by Fonds zur Förderung der wissenschaftlichen Forschung, Austria.

¹⁹Supported by the US Department of Energy, grant DE-FG03-92ER40689.

²⁰Now at School of Operations Research and Industrial Engineering, Cornell University, Ithaca, NY 14853-3801, U.S.A.

²¹Now at University of California at Los Angeles (UCLA), Los Angeles, CA 90024, U.S.A.

1 Introduction

The minimal supersymmetric extension of the Standard Model (SM) requires that the SM particle content is doubled and an extra Higgs $SU(2)_L$ doublet is added. The most general interactions of these particles invariant under the $SU(3)_c \times SU(2)_L \times U(1)_Y$ gauge symmetry are those of the Minimal Supersymmetric Standard Model (MSSM) [1] plus the additional superpotential terms [2]

$$W_{\mathcal{R}_p} = \lambda_{ijk} L_i L_j \bar{E}_k + \lambda'_{ijk} L_i Q_j \bar{D}_k + \lambda''_{ijk} \bar{U}_i \bar{D}_j \bar{D}_k. \quad (1)$$

Here L (Q) are the lepton (quark) doublet superfields, and \bar{D}, \bar{U} (\bar{E}) are the down-like and up-like quark (lepton) singlet superfields, respectively; $\lambda, \lambda', \lambda''$ are Yukawa couplings, and $i, j, k = 1, 2, 3$ are generation indices. The simultaneous presence of the last two terms leads to rapid proton decay, and the solution of this problem in the MSSM is to exclude all terms in Eq.(1) by imposing conservation of R-parity ($R_p = -1^{3B+L+2S}$)¹, a discrete multiplicative quantum number [3]. This solution is not unique, and a number of models [4] predict only a subset of the terms in (1), thus protecting the proton from decay. These alternative solutions are denoted ‘‘R-parity violation’’.

R-parity violation has two major consequences for collider searches. Firstly, the Lightest Supersymmetric Particle (LSP) is not stable and decays to SM particles. Consequently the signatures are very different from the classic missing energy signatures of R-parity conserving models. And secondly, supersymmetric particles (sparticles) can be produced singly via the $LL\bar{E}$ coupling at LEP, either in s-channel resonance [5, 6], or in γe collisions [7], a possibility which is not addressed here. This paper focuses on the pair-production of sparticles, which subsequently decay violating R-parity. Two simplifying assumptions are made throughout the analysis:

- Only one term in Eq.(1) is non-zero. The analysis presented here is restricted to signals from the $LL\bar{E}$ couplings. When the results are translated into limits, it is also assumed that only one of the possible nine λ_{ijk} couplings² is non-zero. The derived limits correspond to the most conservative choice of the coupling.
- The lifetime of the LSP is negligible, i.e. the mean path of flight is less than 1cm.

The second assumption restricts the sensitivity of this analysis in λ , which is however probed well below existing upper-limits from low energy constraints. No assumption on the nature of the LSP is made.

The reported search results use data collected by the ALEPH detector in 1995-1996 at centre-of-mass energies from 130 to 172 GeV. The total data sample used in the analysis corresponds to an integrated recorded luminosity of 27.5 pb⁻¹. The results complement the

¹Here B denotes the baryon number, L the lepton number and S the spin of a field.

²The λ_{ijk} coupling is antisymmetric in the i and j indices, $j > i$ is taken here.

previously reported ALEPH searches for R-parity violating Supersymmetry (SUSY) at LEP 1 energies [8], and the searches for charginos and neutralinos at energies up to 136 GeV [9].

The outline of this paper is as follows: after reviewing the phenomenology of R-parity violating SUSY models and existing limits in Sections 2 and 3, a brief description of the ALEPH detector is given in Section 4. The data and Monte Carlo (MC) samples and the search analyses are described in Sections 5 and 6, and the results and their interpretation within the MSSM are discussed in Section 7. Finally conclusions are drawn in Section 8.

2 Phenomenology

Within minimal Supersymmetry all SM fermions have scalar SUSY partners: the sleptons, sneutrinos and squarks. The SUSY equivalent of the gauge and Higgs bosons are the charginos and neutralinos, which are the mass eigenstates of the $(\tilde{W}^+, \tilde{H}^+)$ and $(\tilde{\gamma}, \tilde{Z}, \tilde{H}_1^0, \tilde{H}_2^0)$ fields, respectively, with obvious notation. The lightest SUSY particle takes a special role in R-parity conserving models: it must be stable [1]. Cosmological arguments [10] then require it to be neutral, and the only possible LSP candidates are the neutralino, the sneutrino and the gravitino.

If R-parity is violated, the LSP can decay to SM particles, and the above cosmological arguments do not apply. The LSP candidates relevant to this analysis are the neutralino, the chargino, the sleptons and the sneutrinos. Squark LSPs are not considered, since they cannot decay directly via the purely leptonic $LL\bar{E}$ operator, and would instead have to undergo a 4-body decay, thus acquire a substantial lifetime and fall outside the assumption of negligible lifetime. It is also assumed that gravitinos are heavy enough to effectively decouple. Gluinos, which cannot be the LSP if the gaugino masses are universal at the GUT scale [1], are assumed to be heavy enough to play no role for the phenomenology at LEP.

The production cross sections do not depend on the size of the R-parity violating Yukawa coupling λ , since the pair-production of sparticles only involves gauge couplings³. The sparticle decay modes are classified according to their topologies: all decays proceeding via the lightest neutralino are throughout referred to as the “indirect” decay modes. The final states produced by the other decays, the “direct” decay modes, consist of two or three leptons as summarised in Table 1. Fig. 1a and b show examples of direct selectron and electron-sneutrino decays, Fig. 1c and d show examples of a direct chargino decay and a neutralino decay via slepton exchange. Note that the classification into direct decay modes is made on the basis of the topology of the decay, and it is therefore immaterial whether the exchanged slepton (or sneutrino) in the chargino or neutralino decays is real or virtual.

The branching ratios of the direct to indirect decay modes explicitly depend on the *a priori* unknown size of the Yukawa coupling λ , the masses and couplings of the decaying sparticle and the lighter SUSY states, and the nature of the LSP [11]. For example,

³Ignoring t-channel processes in which the R-parity violating coupling appears twice.

Sparticle	Decay Mode (λ_{ijk})
χ^+	$\nu_i \nu_j l_k^+, l_i^+ l_j^+ l_k^-, l_i^+ \nu_j \nu_k, \nu_i l_j^+ \nu_k$
χ	$\bar{\nu}_i l_j^+ l_k^-, \bar{\nu}_j l_i^+ l_k^-, \nu_i l_j^- l_k^+, \nu_j l_i^- l_k^+$
\tilde{l}_{iL}^-	$\nu_j l_k^-$
\tilde{l}_{kR}^-	$\nu_i l_j^-, \nu_j l_i^-$
$\tilde{\nu}_i$	$l_j^- l_k^+$

Table 1: *Direct R-parity violating decay modes for a non-zero coupling λ_{ijk} . Here i, j, k are generation indices. For example, the electron sneutrino can decay via the coupling λ_{123} to $\tilde{\nu}_e \rightarrow \mu^- \tau^+$.*

charginos dominantly decay directly if the sleptons and sneutrinos are lighter than the lightest neutralino⁴, independent of the size of the coupling λ . If the masses of the sleptons or sneutrinos lie between the mass of the chargino and the lightest neutralino, the direct decays of charginos can dominate for large values of the R-parity violating coupling and if the neutralino couples higgsino-like. In another example the direct decays of right-handed sleptons can dominate even when the neutralino is the LSP provided the R-parity violating coupling is large and the neutralino couples higgsino-like. In order to be as model independent as possible, all topologies arising from both classes of decays are considered in the subsequent analyses.

Following the above terminology, the lightest neutralino can decay *directly* to two leptons⁵ and a neutrino, either via 2-body decays to lighter sleptons or sneutrinos, or via a 3-body decay. The flavours of the decay products of the neutralino depend on the flavour structure of the Yukawa coupling λ_{ijk} . Heavier neutralinos can also decay *indirectly* to the lightest neutralino: $\chi' \rightarrow \tilde{f} f' \chi$.

The chargino can decay *indirectly* to the neutralino: $\chi^+ \rightarrow \tilde{f} f' \chi$. The chargino can also decay *directly* to SM particles: $\chi^+ \rightarrow l^+ l^- l^+$ or $\chi^+ \rightarrow \nu \nu l^+$. This typically happens when the sleptons/sneutrinos are lighter than the chargino, or when the chargino is the LSP. Throughout this paper the gauge unification condition [1]

$$M_1 = \frac{5}{3} \tan^2 \theta_W M_2 \quad (2)$$

is assumed. Under this assumption the chargino cannot be the LSP if $M_{\chi^+} > 45 \text{ GeV}/c^2$ – the LEP 1 chargino mass limit [8]–, but it is noted that the search analyses cover chargino LSP topologies.

Sleptons and sneutrinos can decay *indirectly* to the lightest neutralino: $\tilde{l} \rightarrow l \chi$ and $\tilde{\nu} \rightarrow \nu \chi$. If the chargino is lighter than the sleptons or sneutrinos, the decays $\tilde{l} \rightarrow \nu \chi^+$

⁴In some particular cases, a subset of the direct decays of the gauginos are not possible with a single non-zero coupling λ_{ijk} since gauginos can decay to sleptons (or sneutrinos) of *all three* flavours. In these instances at least two couplings must be non-zero, although one of the couplings may be much smaller than the other.

⁵In the following the term “lepton” shall denote “charged lepton”.

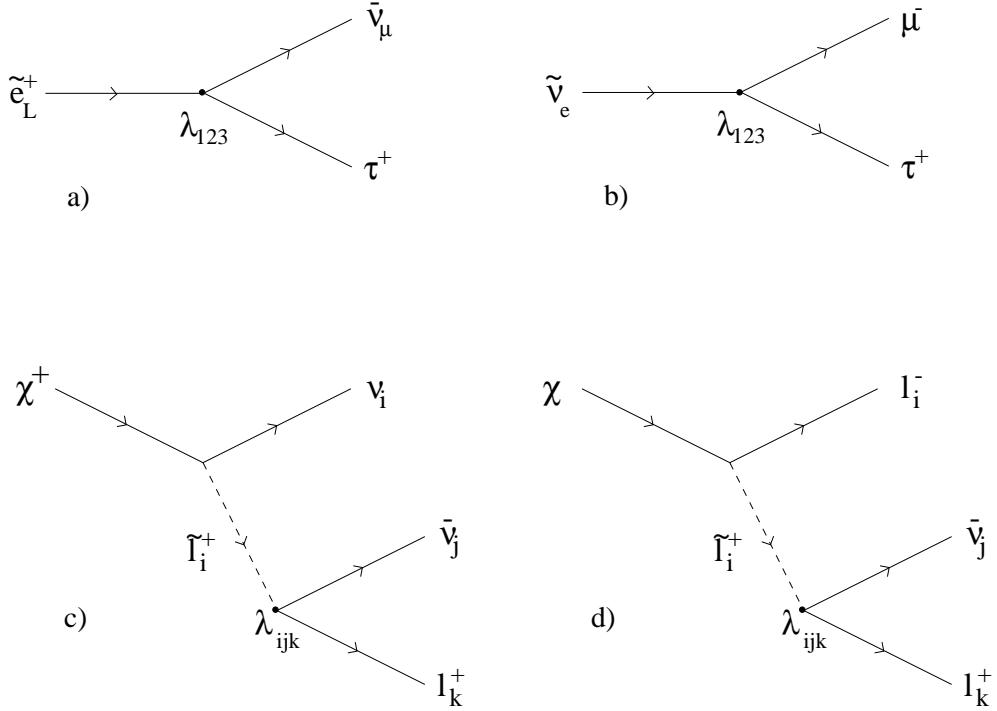


Figure 1: *Examples of R-parity violating decays of (a) left-handed selectrons and (b) electron-sneutrinos via the coupling λ_{123} , and c) charginos and d) neutralinos via slepton exchange.*

and $\tilde{\nu} \rightarrow l^- \chi^+$ are viable decay modes. In the following the decays to charginos are not considered, since the chargino mass limit derived in Section 7.1 is beyond the slepton and sneutrino masses of interest to this analysis. If the sleptons or sneutrinos are the LSPs, pairs of sleptons can decay *directly* to acoplanar leptons, and pairs of sneutrinos to four-lepton final states.

Stops and sbottoms are the most likely candidates for the lightest scalar quark states because of the potential for large mixing angles between the left and right handed states, and because of the large Yukawa couplings of the third generation quarks. They can decay *indirectly* to the lightest neutralino: e.g. $\tilde{t} \rightarrow c\chi$, $\tilde{b} \rightarrow b\chi$. For the decays to the chargino similar remarks apply as for the sleptons and sneutrinos. The squarks cannot decay *directly* to SM particles at tree level via the purely leptonic $LL\bar{E}$ coupling.

3 Existing Limits and the LSP Decay Length

The lower limits on sparticle masses from precision measurements of the Z-width and direct searches at LEP 1 [8] are: $M_{\chi^+}, M_{\tilde{t}}, M_{\tilde{\nu}} > M_Z/2$, and $M_{\tilde{t}}, M_{\tilde{b}} > M_Z/2$ for negligible mixing between left-right squark states, and $M_{\tilde{t}} > 41 \text{ GeV}/c^2$ in the most conservative mixing

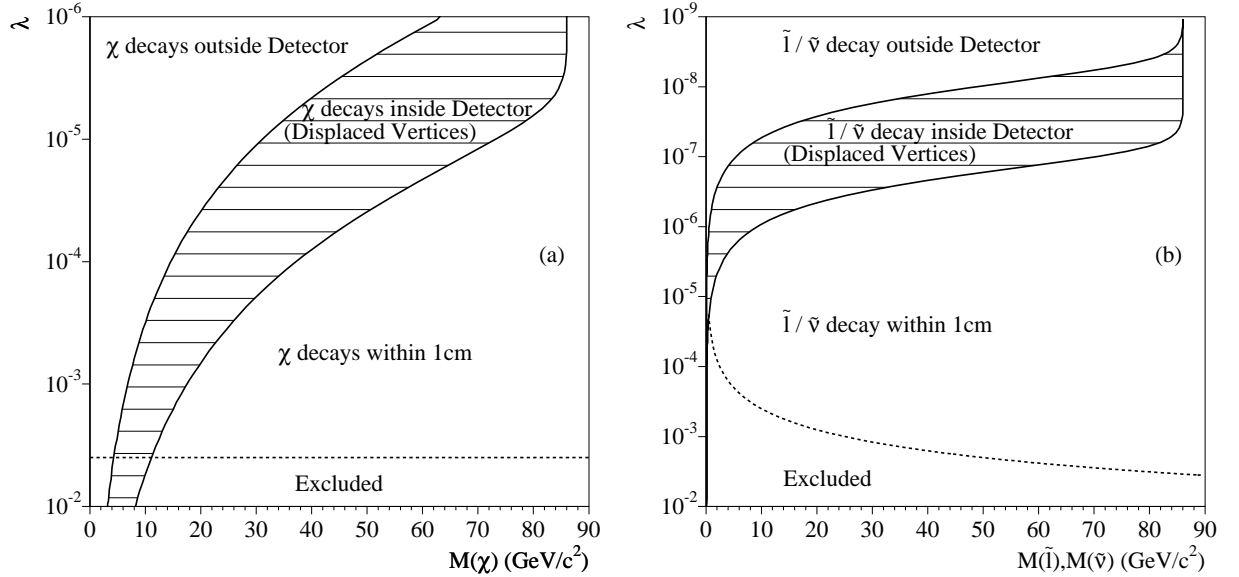


Figure 2: Regions in the (\tilde{M}, λ) -plane where pair-produced LSPs at $\sqrt{s} = 172$ GeV have a mean decay length of $X < 1$ cm, $1 \text{ cm} < X < 3$ m (displaced vertices), and $3 \text{ m} < X$ (LSP decays outside detector) for a) neutralinos (with $M_{\tilde{f}} = 100 \text{ GeV}/c^2$) and b) sleptons and sneutrinos. The dashed lines show the low energy limit on λ_{133} from Eq.(3).

scenario ($\phi_{mix}^{\tilde{t}} = 56^\circ$). Furthermore, from the ALEPH searches at $\sqrt{s} = 130\text{--}136$ GeV (LEP 1.5) $M_{\chi^+} > 65 \text{ GeV}/c^2$ [9], assuming the lightest neutralino to be the LSP.

In addition to the above SUSY mass limits, upper-bounds on the size of the coupling λ from low energy constraints exist [5]. The most stringent limit requires [13]:

$$\lambda_{133} < 0.004 \left(\frac{M_{\tilde{f}}}{100 \text{ GeV}/c^2} \right) \quad (3)$$

The coupling strength determines the mean decay length X of the *direct* decays of the LSP, which is given by [14]

$$\begin{aligned} X_\chi(\text{cm}) &= 0.3 \lambda^{-2} \left(\frac{M_{\tilde{f}}}{100 \text{ GeV}/c^2} \right)^4 \left(\frac{\text{GeV}/c^2}{M_\chi} \right)^5 (\beta\gamma), \\ X_{\tilde{l}}, X_{\tilde{\nu}}(\text{cm}) &= 10^{-12} \lambda^{-2} \left(\frac{\text{GeV}/c^2}{M_{\tilde{l}, \tilde{\nu}}} \right) (\beta\gamma), \end{aligned} \quad (4)$$

for neutralino and slepton/sneutrino decays, respectively, where the Lorentz factor $\beta\gamma = p/M$. Fig. 2 shows regions where the LSP decays within $X < 1$ cm, i.e. the region applicable to this analysis, together with the limit from Eq.(3). Also indicated in Fig. 2 are the regions where the LSP decays within the detector but with a mean decay length exceeding

1 cm, therefore producing displaced vertices, and regions where the LSP decays outside the detector. In the latter case the signatures are identical to the R-parity conserving signals if the LSP is neutral and weakly interacting (neutralino, sneutrino), or they resemble heavy stable charged particle signatures if the LSP is charged (slepton, chargino).

The assumption of negligible lifetime restricts the sensitivity of this analysis to neutralino masses exceeding $M_\chi \gtrsim 10 \text{ GeV}/c^2$. Close to the kinematic limit, gauginos can be probed down to $\lambda \gtrsim 10^{-5}$ for $M_{\tilde{f}} = 100 \text{ GeV}/c^2$, and sleptons and sneutrinos down to $\lambda \gtrsim 10^{-7}$.

4 The ALEPH Detector

The ALEPH detector is described in detail in Ref. [15]. An account of the performance of the detector and a description of the standard analysis algorithms can be found in Ref. [16]. Here, only a brief description of the detector components and the algorithms relevant for this analysis is given.

The trajectories of charged particles are measured with a silicon vertex detector, a cylindrical drift chamber, and a large time projection chamber (TPC). They are immersed in a 1.5 T axial field provided by a superconducting solenoidal coil. The electromagnetic calorimeter (ECAL), placed between the TPC and the coil, is a highly segmented sampling calorimeter which is used to identify electrons and photons and to measure their energy. The luminosity monitors extend the calorimetric coverage down to 24 mrad from the beam axis. An additional shielding against beam related background installed before the 1996 running reduces the acceptance by 10 mrad. The hadron calorimeter (HCAL) consists of the iron return yoke of the magnet instrumented with streamer tubes. It provides a measurement of hadronic energy and, together with the external muon chambers, muon identification.

The calorimetry and tracking information are combined in an energy flow algorithm, classifying a set of energy flow “particles” as photons, neutral hadrons and charged particles. Hereafter, charged particle tracks reconstructed with at least four hits in the TPC, and originating from within a cylinder of length 20 cm and radius 2 cm coaxial with the beam and centred at the nominal collision point, will be referred to as *good tracks*.

Lepton identification is described in [16]. Electrons are identified using the transverse and longitudinal shower shapes in ECAL. Muons are separated from hadrons by their characteristic penetrating pattern in HCAL and the presence of hits in the muon chambers.

5 Data and Monte Carlo Samples

This analysis uses data collected by ALEPH in 1996 at centre-of-mass energies of 161.3 GeV (11.1 pb^{-1}), 170.3 GeV (1.1 pb^{-1}) and 172.3 GeV (9.6 pb^{-1}). In the search for sfermions the

sensitivity is increased by including also the LEP 1.5 data recorded in 1995 at $\sqrt{s} = 130\text{--}136$ GeV (5.7 pb^{-1}).

For the purpose of designing selections and evaluating efficiencies, samples of signal events for all accessible final states have been generated using **SUSYGEN** [17] for a wide range of signal masses. A subset of these has been processed through the full **ALEPH** detector simulation and reconstruction programs, whereas efficiencies for intermediate points have been interpolated using a fast, simplified simulation.

For the stop, the decays via loop diagrams to a charm quark and the lightest neutralino result in a lifetime larger than the typical hadronisation time scale. The scalar bottom can also develop a substantial lifetime in certain regions of parameter space. This has been taken into account by modifying the **SUSYGEN** MC program to allow stops and sbottoms to hadronise prior to their decays according to the spectator model [18].

Samples of all major backgrounds have been generated and passed through the full simulation, corresponding to at least 20 times the collected luminosity in the data. Events from $\gamma\gamma \rightarrow \text{hadrons}$, $e^+e^- \rightarrow q\bar{q}$ and four-fermion events from $W e\nu$, $Z\gamma^*$ and Zee were produced with **PYTHIA** [19], with an invariant mass cut for the resonance of $0.2\text{ GeV}/c^2$ for $Z\gamma^*$ and $W e\nu$, and $2\text{ GeV}/c^2$ for Zee . Pairs of W bosons were generated with **KORALW** [20]. Pair production of leptons was simulated with **UNIBAB** [21] (electrons) and **KORALZ** [22] (muons and taus), and the process $\gamma\gamma \rightarrow \text{leptons}$ with **PHOT02** [23].

6 Selection Criteria

The topologies expected from sparticle pair production decaying via a dominant $LL\bar{E}$ coupling share the signature of leptons in the final state. They can consist of as little as two acoplanar leptons in the simplest case, or they may consist of as many as six leptons plus four neutrinos in the most complicated case. In addition to the purely leptonic topologies, the cascade decays of squarks or heavier gauginos into lighter gaugino states may produce multi-jet and multi-lepton final states.

In the following sections the selections of the various topologies are described in turn. A brief summary of all selections, the expected number of background events from SM processes, and the number of candidates selected in the data is shown in Table 2. The positions of the most important cuts of all selections have been chosen such that the expected upper limit (\tilde{N}_{95}) without the presence of a signal is minimised [24]. This minimum was determined using the Monte Carlo for background and signal, focussing on signal masses close to the high end of the sensitivity region.

6.1 Six Leptons

Six lepton topologies are expected from the production of pairs of charginos, which decay via sneutrinos into three leptons each. To select this topology the analysis requires at least

Selection	signal process	Background	Data
Six Leptons	$\chi^+\chi^- \rightarrow \text{llllll}$	0.02	0
Six Leptons plus \cancel{E}	$\chi^+\chi^- \rightarrow \text{l}\nu\text{l}\nu\chi\chi \rightarrow \text{l}\nu\text{l}\nu\text{ll}\nu\text{ll}\nu$ $\chi^+\chi^- \rightarrow \text{l}\nu\chi\text{lll} \rightarrow \text{l}\nu\text{ll}\nu\text{lll}$ $\chi'\chi \rightarrow \text{ll}\chi\chi \rightarrow \text{llll}\nu\text{ll}\nu$ $\tilde{\ell}\tilde{\ell} \rightarrow \text{l}\chi\text{l}\chi \rightarrow \text{lll}\nu\text{ll}\nu$	0.12	0
Four Leptons	$\tilde{\nu}\tilde{\nu} \rightarrow \text{llll}$	0.90	0
Four Leptons plus \cancel{E}	$\chi\chi \rightarrow \text{ll}\nu\text{ll}\nu$ $\chi'\chi \rightarrow \nu\nu\chi\chi \rightarrow \nu\nu\text{ll}\nu\text{ll}\nu$ $\tilde{\nu}\tilde{\nu} \rightarrow \nu\chi\nu\chi \rightarrow \nu\text{ll}\nu\text{ll}\nu$ $\tilde{\nu}\tilde{\nu} \rightarrow \nu\chi\text{ll} \rightarrow \nu\text{ll}\nu\text{ll}$ $\tilde{\ell}\tilde{\ell} \rightarrow \text{l}\chi\text{l}\nu \rightarrow \text{lll}\nu\text{l}\nu$ $\chi^+\chi^- \rightarrow \text{l}\nu\chi\text{l}\nu\nu \rightarrow \text{l}\nu\text{ll}\nu\text{l}\nu\nu$ $\chi^+\chi^- \rightarrow \text{l}\nu\nu\text{lll}$ $\tilde{\ell}\tilde{\ell} \rightarrow \text{l}\nu\text{l}\nu$	0.47	1
Acoplanar Leptons	$\chi^+\chi^- \rightarrow \text{l}\nu\nu\text{l}\nu\nu$	12 ^(*)	15
Leptons and Hadrons	$\chi^+\chi^- \rightarrow \text{qqqq}\chi\chi \rightarrow \text{qqqqll}\nu\text{ll}\nu$ $\chi^+\chi^- \rightarrow \text{qq}\text{l}\nu\chi\chi \rightarrow \text{qq}\text{l}\nu\text{ll}\nu\text{ll}\nu$ $\chi^+\chi^- \rightarrow \text{qq}\chi\text{lll} \rightarrow \text{qqll}\nu\text{lll}$ $\chi^+\chi^- \rightarrow \text{qq}\chi\text{l}\nu\nu \rightarrow \text{qqll}\nu\text{l}\nu\nu$ $\chi'\chi \rightarrow \text{qq}\chi\chi \rightarrow \text{qqll}\nu\text{ll}\nu$ $\tilde{\text{q}}\tilde{\text{q}} \rightarrow \text{q}\chi\text{q}\chi \rightarrow \text{qll}\nu\text{qll}\nu$	1.43	1

Table 2: *The selections, the signal processes giving rise to the above topologies, the number of background events expected, and the number of candidate events selected in the data ($\sqrt{s} = 130 - 172$ GeV). The value marked (*) contains 10.3 events of irreducible background from WW production.*

five, but no more than nine good tracks, of which at least four should be identified as leptons (i.e. electrons or muons). To ensure that the tracks are well separated, the event is clustered into four (and three) jets using the Durham algorithm, and a minimum Durham scale y_4 of 0.002 (and y_3 of 0.01) is required between all the jets. After this, a total background of 0.02 events is expected, predominantly coming from $e^+e^- \rightarrow Ze^+e^-$.

6.2 Six Leptons plus Missing Energy

This topology is expected from the indirect decays of charginos, neutralinos and sleptons. The selection requires a visible mass of at least $25 \text{ GeV}/c^2$ and at least five, but no more than eleven good tracks, with at least two of them identified as leptons. Fig. 3a shows the distribution of the number of identified leptons N_{lep} for data, background Monte Carlo and events from $\chi^+\chi^- \rightarrow l\nu l\nu l\nu l\nu$ at an intermediate stage of the selection. In addition the amount of neutral hadronic energy is limited to $6\%\sqrt{s}$ and 17% of the total energy of all good tracks. Since missing energy is expected for the signal, the events should have a visible mass of less than $85\%\sqrt{s}$ and a minimum missing transverse momentum of $2\%\sqrt{s}$. The remaining background from $q\bar{q}$ and $\tau^+\tau^-$ is reduced by requiring y_4 to be at least 0.004. The total background after all cuts amounts to 0.12 events expected in the data, mainly consisting of events from $q\bar{q}$, $Z\gamma^*$ and Ze^+e^- .

6.3 Four Leptons

A final state of four leptons is expected from the direct decays of pairs of sneutrinos. For the purpose of defining selections, the possible lepton flavour combinations ($l_i l_k l_i l_k$ or $l_j l_k l_j l_k$) can be divided into three classes according to the number of taus: final states with no taus, two taus or four taus. For all cases a common preselection is applied, requiring a visible mass of at least $30 \text{ GeV}/c^2$ and four, five or six good tracks in the event. To reject background from $\tau^+\tau^-$, events are clustered into jets, which should be well separated ($y_4 > 4 \times 10^{-4}$ and $y_3 > 0.007$) and contain at least one good track. The discriminating power of y_4 is illustrated in Fig. 3b, comparing the distribution for data, background Monte Carlo and events from direct sneutrino decays.

For a signal with four taus, the remaining background is reduced further by requiring that no energy be reconstructed in a cone of 12° around the beam axis. This cut introduces an inefficiency due to beam related background and electronic noise, which was measured to be 0.5% (4%, 2%) at centre-of-mass energy of 130–136 (161, 172) GeV, using events triggered at random beam crossings. In addition, the amount of neutral hadronic energy E_{had} should be less than 30% of the visible energy.

The requirements on E_{had} and energies at low angles can be dropped for signal final states with two taus (no taus) by introducing new requirements on the lepton content of the event: there should be no conversions reconstructed and two muons or electrons identified (at least three leptons identified), with a total leptonic energy E_{lep} fulfilling $E_{\text{had}} < 30\%E_{\text{lep}}$

($< 15\%E_{\text{lep}}$). For two taus, a missing transverse momentum of at least $2\%\sqrt{s}$ can be required to suppress the remaining background, whereas for no taus, events should have less than $25\text{ GeV}/c$ of missing momentum along the beam axis.

For the case of two or more non-zero Yukawa couplings, final states with an odd number of taus are accessible in sneutrino pair production. Since the four tau selection contains no cut on leptonic energy, such final states are selected at least as efficiently as four tau final states.

The total background expected by the inclusive combination of all three subselections amounts to 0.90 events. Most of this background consists of events from $Z\gamma^*$ and Ze^+e^- .

6.4 Four Leptons plus Missing Energy

A final state with four leptons of arbitrary flavour and missing energy can be produced in decays of charginos, neutralinos, sleptons and sneutrinos (Table 2). It is selected using criteria similar to the ones defined for the four-lepton final states: events should have four, five or six good tracks, of which at least one should correspond to an identified electron or muon. A total visible mass of at least $16\text{ GeV}/c^2$ and a missing transverse momentum of more than $5\text{ GeV}/c$ is required. The total neutral hadronic energy in the event should be less than the total leptonic energy. The remaining background from $q\bar{q}$ and $\tau^+\tau^-$ is reduced further by requiring y_4 to be greater than 6×10^{-4} . In addition, events are clustered into jets using the JADE algorithm and a y_{cut} of m_τ^2/s to form tau-like jets, at least four of which are required to contain good tracks. After these cuts, a background of 0.47 events is expected in the total data sample, mainly consisting of four-fermion events.

6.5 Acoplanar Leptons

Final states with two leptons and missing energy are expected from direct decays of sleptons and charginos. Depending on the process and the generation structure of the $LL\bar{E}$ operator, the charged leptons can be of equal flavour (e.g. left-handed sleptons) or of arbitrary flavour (charginos). Selections for the topology of two acoplanar leptons have already been developed for the search for sleptons under the assumption that R-parity is conserved: for $\sqrt{s} = 130\text{--}136\text{ GeV}$, the selection described in [25] is used, whereas for $\sqrt{s} = 161\text{--}172\text{ GeV}$ the analysis published in [26] is extended to allow for mixed lepton flavours.

For $e\mu$ final states, the requirement for two identified leptons of the same flavour is replaced by the requirement for one electron and one muon. For $e\tau$ ($\mu\tau$), the leading lepton should be an electron (muon) with momentum less than $75\text{ GeV}/c$. In case there is a second lepton identified, its momentum should be less than $30\text{ GeV}/c$ at $\sqrt{s} = 161\text{ GeV}$ ($25\text{ GeV}/c$ at $\sqrt{s} = 172\text{ GeV}$).

All these subselections have irreducible background from leptonic WW events, which is particularly large when the flavour structure of the signal process requires to use inclusive

combinations of the subselections. Therefore subtracting this background using the method suggested in [27] increases the sensitivity of the analysis.

6.6 Leptons and Hadrons

Final states with leptons and hadrons are expected from charginos, neutralinos and squarks decaying to the lightest neutralino. Depending on the masses of the supersymmetric particles and on the lepton flavour composition in the neutralino decays, signal events populate different regions in track multiplicity N_{ch} , visible mass M_{vis} and leptonic energy E_{lep} . As the properties of background events change as a function of these variables, three different subselections have been developed to select the full range of signal events at a small background level (Table 3).

All three subselections are based on the central requirement of large leptonic energy, supplemented with cuts on the amount of neutral hadronic energy E_{had} (Fig. 3c) and non-leptonic energy E_{nonlep} . Due to the presence of at least two neutrinos, signal events are expected to contain some missing momentum. This is used to suppress the background by requiring a minimum missing transverse momentum p_{\perp}^{miss} . Background from hadronic events with energetic initial state radiation photons is reduced by removing events with large missing momentum p_z^{miss} along the beam axis (for photons escaping at small polar angles) or by requiring the charged multiplicity $N_{\text{ch}}^{\text{jet}}$ in all jets found with $y_{\text{cut}} = 0.005$ to be at least one (for photons in the detector). Most of the remaining background is then rejected by selecting spherical events using y_3, y_4, y_5 and the event thrust. At this stage background at $\sqrt{s} = 161\text{--}172$ GeV dominantly comes from $W^+W^- \rightarrow l\nu q\bar{q}$. The kinematic properties of these events can be exploited to suppress the background by defining

$$\chi_{WW}^2 = \left(\frac{m_{qq} - m_W}{10 \text{ GeV}/c^2}\right)^2 + \left(\frac{m_{l\nu} - m_W}{10 \text{ GeV}/c^2}\right)^2 + \left(\frac{p_l - 43 \text{ GeV}/c}{\Delta p_l}\right)^2.$$

Here m_{qq} is the hadronic mass, i.e. the mass of the event after removing the leading lepton, $m_{l\nu}$ is the mass of the leading lepton and the missing momentum, and p_l is the momentum of the leading lepton. The spread Δp_l of lepton momenta from WW is approximated by $5 \text{ GeV}/c$ at $\sqrt{s} = 161$ GeV and $5.8 \text{ GeV}/c$ at $\sqrt{s} = 172$ GeV. As can be seen in Fig. 3d, WW events are likely to occur at small χ_{WW}^2 , and can therefore be rejected by requiring a minimum χ_{WW}^2 for events to be selected.

Subselection I is designed to select final states with large leptonic energy and at least two jets, this way covering most of the parameter space. For charginos decaying to $l\nu q\bar{q}\chi\chi$ with a small mass difference between the chargino and the lightest neutralino, the efficiency is increased with subselection II, concentrating on events with small multiplicity and large leptonic energy fraction. For small masses of the lightest neutralino, signal events tend to have a smaller leptonic energy fraction such that additional cuts on the event shape are needed to suppress the background (subselection III). Final states with hadrons and leptons as expected from chargino, neutralino and squark decays are efficiently selected by using the inclusive combination of all three subselections. The background amounts to 1.43

subselection I	subselection II	subselection III
$N_{\text{ch}} \geq 5$ $25 \text{ GeV}/c^2 < M_{\text{vis}}$	$15 \geq N_{\text{ch}} \geq 5$ $20 \text{ GeV}/c^2 < M_{\text{vis}} < 75\% \sqrt{s}$	$N_{\text{ch}} \geq 11$ $55\% \sqrt{s} < M_{\text{vis}} < 80\% \sqrt{s}$
$p_{\perp}^{\text{miss}} > 3.5\% \sqrt{s}$ $ p_z^{\text{miss}} < 27 \text{ GeV}/c$	$p_{\perp}^{\text{miss}} > 2.5\% \sqrt{s}$	$p_{\perp}^{\text{miss}} > 5\% \sqrt{s}$ $N_{\text{ch}}^{\text{jet}} \geq 1$
$y_5 > 0.006$	$y_3 > 0.009$ $y_4 > 0.0026$	$y_3 > 0.025$ $y_4 > 0.012$ $y_5 > 0.004$ Thrust < 0.85
$N_{\text{lep}} \geq 1$ $E_{\text{nonlep}} < 54\% \sqrt{s}$ $E_{\text{had}} < 28\% E_{\text{vis}}$	$N_{\text{lep}} \geq 1$ $E_{\text{nonlep}} < 70\% \sqrt{s}$ $E_{\text{had}} < 22\% E_{\text{lep}}$	$N_{\text{lep}} \geq 1$ $E_{\text{lep}} > 20\% E_{\text{had}}$
$\chi_{\text{WW}} > 3.3$ (for $\sqrt{s} = 161 \text{ GeV}$), $\chi_{\text{WW}} > 3.5$ (for $\sqrt{s} = 172 \text{ GeV}$)		

Table 3: *The complete list of cuts as defined for the leptons and hadrons selection.*

Topology	ee	$\mu\mu$	$\tau\tau$	$e\mu$	$e\tau$	$\mu\tau$
WW background	1.6	1.7	1.2	3.6	2.3	2.3
Selected in Data	1	1	1	5	3	7

Table 4: *The 15 candidate events selected in the data by the acoplanar lepton selection, listed according to the topology in which they are selected, and the WW background expectation. Some of the background and candidate events are in common to several selections.*

events expected in the total data sample. This background mainly consists of events from $q\bar{q}(\gamma)$ and W pair production.

7 Results

In the data recorded at $\sqrt{s} = 130\text{--}172 \text{ GeV}$, corresponding to an integrated luminosity of 27.5 pb^{-1} , a total of 17 events is selected. This is in agreement with the expectation from Standard Model backgrounds of 14.5 events. Out of these, 15 events are selected by the acoplanar lepton selection, with a subtractable background from $W^+W^- \rightarrow l\nu l\nu$ of 10.3 events. All of these events show clear characteristics of WW-events, and are split up into the different lepton flavours as shown in Table 4. The highest number of candidates is observed in the $\mu\tau$ channel (seven candidates with a total expected background of 2.6), which also shares two candidates with the $e\mu$ channel. The probability for seeing such an upwards fluctuation in any of the six channels is $\sim 10\%$.

The other two events are selected by the “four leptons plus missing energy” selection and the “leptons and hadrons” selection, respectively. The former is consistent with coming from $e^+e^- \rightarrow Z\gamma^* \rightarrow e^+e^-\tau^+\tau^-$, whereas the latter can be interpreted as $W^+W^- \rightarrow e\nu q\bar{q}$.

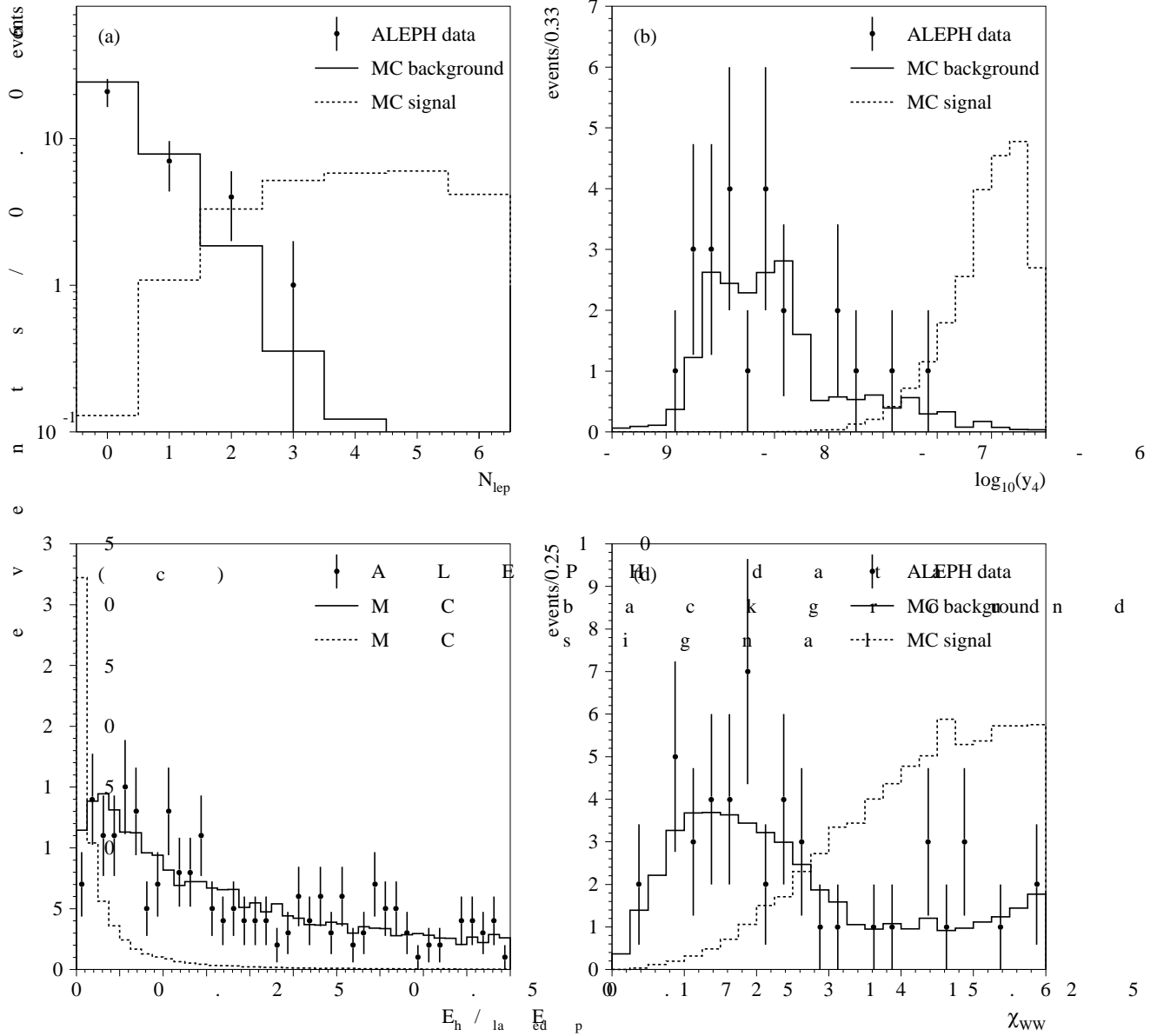


Figure 3: The distributions of a) number of identified leptons N_{lep} as used in the “Six Lepton plus Missing Energy” selection b) y_4 as used in the “Four Lepton” selection and c) E_{had}/E_{lep} and d) χ_{WW} as used in the “Leptons and Hadrons” selection. The data (dots) at $\sqrt{s} = 161-172$ GeV are compared to the background Monte Carlo (full histograms). The dashed histograms show typical signal distributions in arbitrary normalisation: a) $\chi^+\chi^- \rightarrow \nu\nu\nu\chi\chi$ for λ_{122} and λ_{133} , b) $\tilde{\nu}\tilde{\nu} \rightarrow llll$ for all couplings, c) and d) $\chi^+\chi^- \rightarrow \nu\nu qq\chi\chi$ or $qqqq\chi\chi$ for λ_{122} and λ_{133} . Only a subset of the cuts is applied to preserve sufficient statistics.

In the following sections, the absence of any significant excess of events in the data with respect to the Standard Model expectation is used to set limits on the production of charginos and neutralinos, sleptons, sneutrinos and squarks. The systematic error on the efficiencies is of the order of 3%, dominated by the statistical uncertainty due to limited Monte Carlo statistics, with small additional contributions from lepton identification and energy flow reconstruction. It is taken into account by conservatively reducing the selection efficiency by one standard deviation.

7.1 Charginos and Neutralinos

Charginos and heavier neutralinos can decay either *indirectly* via the lightest neutralino, or *directly* via (possibly virtual) sleptons or sneutrinos. The corresponding branching fractions of the direct and indirect decays, as well as the branching fractions of the direct decays into different leptonic final states (c.f. Table 1) in general depend on the field content and masses of the charginos and neutralinos, the sfermion mass spectrum and the Yukawa coupling λ . Furthermore, because of possible mixing in the third generation sfermion sector, staus, stops and sbottoms can be substantially lighter than their first or second generation partners. The effect of light staus is to increase the tau branching ratio in the indirect decays (e.g. $\chi^+ \rightarrow \tau\nu\chi$) with respect to the other indirect decay modes, whereas light stops and sbottoms increase the hadronic branching ratios of the indirect decays. Light staus can also affect the BRs of the direct decay modes, increasing the BRs to e, μ or τ final states depending on the generation structure of the R-parity violating couplings.

To constrain a model with such a large number of unknown parameters, limits were set that are independent of the various branching ratios. For this purpose, the signal topologies are classified into three distinct cases: the *direct topologies* (when both charginos decay directly), the *indirect topologies* (when both charginos decay indirectly), and the *mixed topologies* (when one chargino decays directly, one indirectly). Secondly, the branching ratios of the various decays involved in both indirect and direct decays are varied freely, and the limit is set using the most conservative choice.

Limits have been evaluated in the framework of the MSSM, where the masses of the gauginos can be calculated from the three parameters M_2, μ and $\tan\beta$. The cross sections of neutralinos (charginos) receive a positive (negative) contribution due to t-channel selectron (electron-sneutrino) exchange, respectively, and thus depend also on $m_{\tilde{l}}$ and $m_{\tilde{\nu}}$. A common slepton and sneutrino mass m_0 at the GUT scale was assumed, which according to the renormalisation group equations [28] links the slepton and sneutrino masses at the electroweak scale by⁶

$$\begin{aligned}
m_{\tilde{l}_R}^2 &= m_0^2 + 0.22 M_2^2 - \sin^2 \theta_W M_Z^2 \cos 2\beta \\
m_{\tilde{l}_L}^2 &= m_0^2 + 0.75 M_2^2 - \frac{1}{2}(1 - 2 \sin^2 \theta_W) M_Z^2 \cos 2\beta \\
m_{\tilde{\nu}}^2 &= m_0^2 + 0.75 M_2^2 + \frac{1}{2} M_Z^2 \cos 2\beta.
\end{aligned}
\tag{5}$$

⁶Ignoring effects from the R-parity violating couplings.

In summary, the limits derived in this approach are independent of the branching ratios of the gauginos, and only depend on the four parameters $M_2, \mu, \tan \beta, m_0$, which determine the masses and the cross sections of the charginos and neutralinos. Therefore the limits are by construction valid for any size or generation structure of the R-parity violating coupling λ , they apply for neutralino, slepton or sneutrino LSPs alike, and are independent of mixing between the third generation sfermions. It should be noted that the branching ratios which set the limit may not correspond to a physically viable model in certain cases (i.e. in specific points in parameter space $M_2, \mu, \tan \beta, m_0$), and hence the real limit within a specific model may be even stronger than the conservative and more general limit presented in this section.

As discussed in Section 3, the lightest neutralino can have a decay length of more than 1 cm when $m_\chi \lesssim 10 \text{ GeV}/c^2$ for couplings which are not already excluded by low energy constraints. Since long-lived sparticles are not considered in this analysis, regions in parameter space with $m_\chi < 10 \text{ GeV}/c^2$ are ignored in the following. Limits on the charginos and neutralinos are derived in Sections 7.1.1 and 7.1.2 for the two extreme cases of 100% indirect and 100% direct topologies, respectively, and the intermediate case of mixed topologies is investigated in Section 7.1.3. Due to the large cross section for pair production of charginos, the data recorded at $\sqrt{s} = 130\text{--}136 \text{ GeV}$ do not improve the sensitivity of the analysis, and therefore have not been included here.

7.1.1 Dominance of indirect decays

In this scenario all charginos and neutralinos are assumed to decay to the lightest neutralino, which then decays violating R-parity into two charged leptons and a neutrino. The indirect topologies generally correspond to the cases where the sleptons and sneutrinos are heavier than the charginos and the neutralinos. When the sleptons or sneutrinos are lighter than the charginos (or the heavier neutralinos) and heavier than the lightest neutralino, the indirect decays will also dominate provided that the neutralino couples gaugino-like and/or the coupling λ is small.

For charginos the “Leptons and Hadrons” selection is combined with the “Six Leptons plus Missing Energy” selection, and for neutralinos ($\chi\chi$) and ($\chi'\chi$) the inclusive combination of the “Leptons and Hadrons” and the “Four and Six Leptons plus Missing Energy” analyses was used. Signal efficiencies were determined as a function of $M_{\chi^+}, M_{\chi'}, M_\chi$ and the choice of generation indices i, j, k of the coupling λ_{ijk} . In general, efficiencies scale with the mass of the lightest neutralino, and become smaller with decreasing neutralino mass. Final states with a large number of electrons or muons are selected with high efficiencies compared to processes involving hadronic decays or couplings allowing the lightest neutralino to decay into taus. A set of efficiencies for choices of the lepton flavour corresponding to the smallest efficiencies is shown in Table 5. The efficiencies used for setting limits were checked to give a conservative estimate for two-body decay cascades via light sfermions as well as three-body decays of charginos and neutralinos.

For a given value of m_0 and $\tan \beta$, limits are derived in the (μ, M_2) plane for the worst case in terms of third generation mixing angles and the lepton flavour composition of the

Signal Process	Topology	Masses (GeV/c ²)	Efficiency (%)
$\chi^+\chi^- \rightarrow W^*W^*\tau\tau\nu\tau\nu$	indirect	$m_{\chi^+} = 85, m_{\chi} = 30$	40
		$m_{\chi^+} = 85, m_{\chi} = 70$	48
$\chi^+\chi^- \rightarrow e\tau\tau e\tau\tau$	direct	$m_{\chi^+} = 85$	73
$\chi^+\chi^- \rightarrow \tau\nu\nu\tau\nu\nu$	direct	$m_{\chi^+} = 85$	44
$\chi^+\chi^- \rightarrow \tau\nu\nu W^*e\tau\nu$	mixed	$m_{\chi^+} = 85, m_{\chi} = 30$	53
$\chi'\chi \rightarrow Z^*\tau\tau\nu\tau\tau\nu$	indirect	$m_{\chi'} = 95, m_{\chi} = 75$	47
$\chi\chi \rightarrow \tau\tau\nu\tau\tau\nu$	direct	$m_{\chi} = 40$	30
$\tilde{\tau}\tilde{\tau} \rightarrow \tau\tau\tau\tau\nu\tau\tau\nu$	indirect	$m_{\tilde{\tau}} = 50, m_{\chi} = 30$	62
		$m_{\tilde{\tau}} = 50, m_{\chi} = 10$	51
$\tilde{\ell}\tilde{\ell} \rightarrow \tau\nu\tau\nu$	direct	$m_{\tilde{\ell}} = 50$	37
$\tilde{\tau}\tilde{\tau} \rightarrow \tau\nu\tau\tau\tau\nu$	mixed	$m_{\tilde{\tau}} = 50, m_{\chi} = 30$	46
$\tilde{\nu}\tilde{\nu} \rightarrow \nu\nu\tau\tau\nu\tau\tau\nu$	indirect	$m_{\tilde{\nu}} = 50, m_{\chi} = 30$	41
		$m_{\tilde{\nu}} = 50, m_{\chi} = 10$	12
$\tilde{\nu}\tilde{\nu} \rightarrow \tau\tau\tau\tau$	direct	$m_{\tilde{\nu}} = 50$	42
$\tilde{\nu}\tilde{\nu} \rightarrow \tau\tau\nu\tau\tau\nu$	mixed	$m_{\tilde{\nu}} = 50, m_{\chi} = 30$	50
$\tilde{t}\tilde{t} \rightarrow c\bar{c}\tau\tau\nu\tau\tau\nu$	indirect	$m_{\tilde{t}} = 50, m_{\chi} = 30$	19

Table 5: Selection efficiencies at $\sqrt{s} = 172$ GeV for a representative set of signal processes, with a lepton flavour composition in the final state leading to the smallest efficiencies.

final state. In most points this worst case is identified as $(ijk)=(133)$ with $\chi \rightarrow \tau\tau\nu$, corresponding to a maximum number of taus in the final state, with small squark masses, leading to a large hadronic branching fraction. The limits set this way are by construction independent of the choice of generation indices or third generation mixing angles.

For each point in $\mu - M_2 - m_0 - \tan\beta$, the \bar{N}_{95} -prescription is applied to decide which combination of chargino and neutralino searches gives the best exclusion power and should therefore be used to set the limit. Fig. 4a shows the limits obtained in the (μ, M_2) plane for a fixed value of $\tan\beta$ and m_0 , from which a lower limit on the chargino and neutralino masses can be derived. Scanning over m_0 , these limits are shown as a function of $\tan\beta$ in Fig. 5. Since the worst case limit is basically set by the purely hadronic decays, the $\tan\beta$ -dependence of the two mass limits is dictated mainly by the relative change of the chargino and neutralino mass isolines in the (μ, M_2) plane with respect to $\tan\beta$.

For small m_0 , contributions from t-channel $\tilde{\nu}$ -exchange suppress the pair production of charginos in the gaugino region. However, according to Eq. 5 selectrons are expected to be light in the same region of parameter space, enhancing the cross section for $\chi\chi$ and $\chi'\chi$ production. In contrast to scenarios with conservation of R-parity, both these processes lead to visible final states, allowing to exclude these regions up to large chargino masses.

At values of $\tan\beta$ close to one, small neutralino masses are excluded by an interplay of limits on $\chi\chi'$ -production from LEP1 [8] and the LEP2 chargino and neutralino limits (Fig. 4b), in the case of $\tan\beta = 1$ still allowing neutralino masses as small as 25 GeV/c².

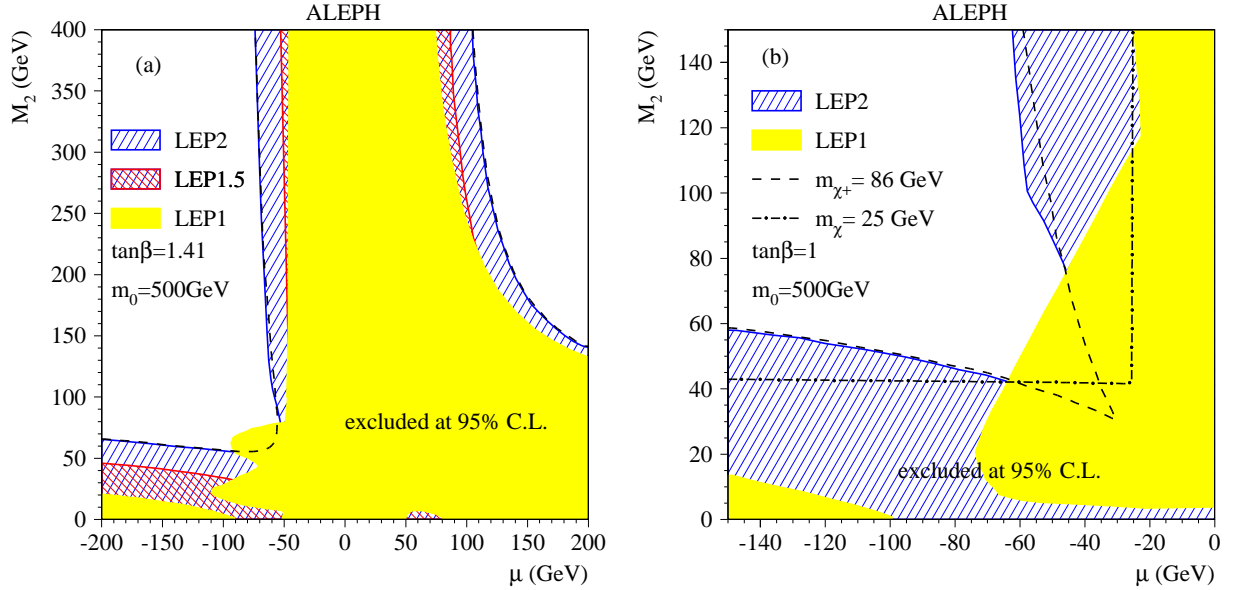


Figure 4: *Regions in the (μ, M_2) plane excluded at 95% C.L. at $m_0 = 500 \text{ GeV}/c^2$ and a) $\tan\beta = 1.41$ or b) $\tan\beta = 1$, assuming that the indirect decays dominate. The superimposed dashed and dash-dotted lines show the kinematic limit $M_{\chi^+} = 86 \text{ GeV}/c^2$, and a fixed neutralino mass of $M_{\chi} = 25 \text{ GeV}/c^2$. The neutralino limit of $M_{\chi} = 25 \text{ GeV}/c^2$ is set at $\tan\beta = 1$ and $(\mu, M_2) \sim (-60, 40)$ by an interplay of the LEP1 and LEP2 exclusion limits.*

7.1.2 Dominance of direct decays

In this scenario the charginos and the heavier neutralinos are assumed to decay directly to SM particles. This generally corresponds to the cases when the sleptons or the sneutrinos are the LSP. Furthermore, when the sleptons or sneutrinos are lighter than the charginos (or the heavier neutralinos) and heavier than the lightest neutralino, the direct decays can dominate provided that the neutralino couples higgsino-like and λ is large.

Charginos can decay either into one charged lepton plus two neutrinos or into three charged leptons, leading to two-, four- or six-lepton topologies. The composition of lepton flavours appearing in these final states depends on the field content of the chargino, the generation indices and the details of the mass spectrum. For simplicity, the inclusive combination of all corresponding selections is used. All branching fractions and flavour compositions have been scanned to identify the overall most conservative limit, which in general is set by charginos decaying dominantly into two taus via a coupling involving all three lepton flavours. For such couplings, selections for all possible flavour combinations have to be combined, leading to the largest possible background and number of candidate events. If in addition the branching fraction into two taus is large, selection efficiencies are smallest, resulting in the most conservative limit.

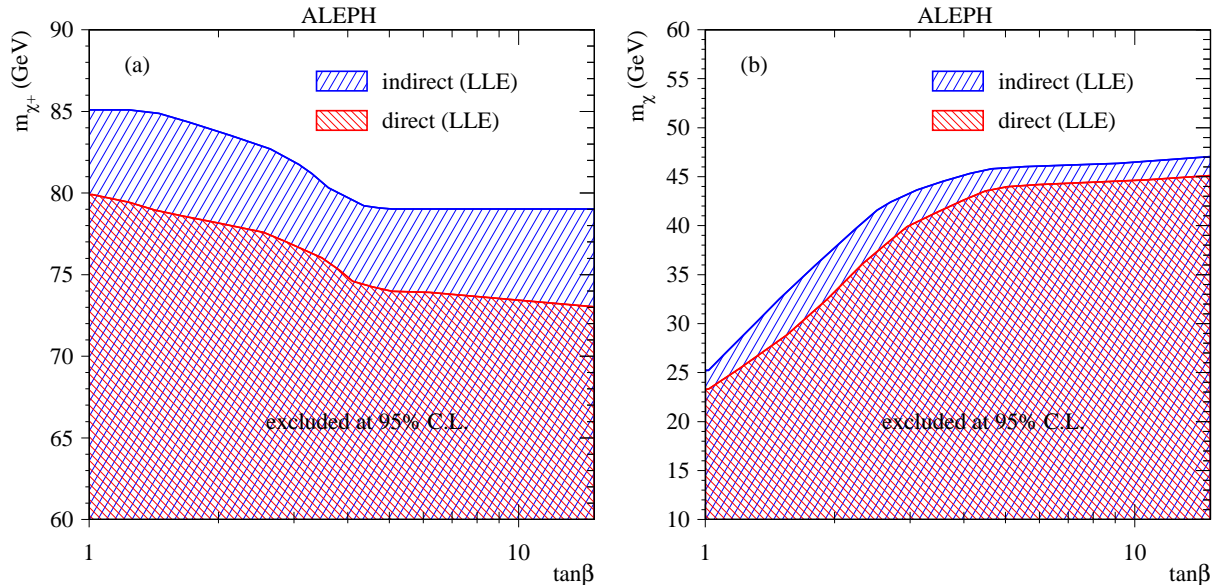


Figure 5: The 95% C.L. limit on a) the chargino mass and b) the lightest neutralino mass as a function of $\tan\beta$, assuming the dominance of either direct or indirect decay modes. The limits hold for any choice of μ , M_2 , m_0 and the generation indices i, j, k of the coupling λ_{ijk} .

For the scenario considered here, all neutralinos are assumed to decay to two charged leptons plus a neutrino. Using the “Four Leptons plus missing Energy” selection, efficiencies have been calculated as a function of the neutralino masses for each possible flavour composition in the final state. As before, the smallest efficiency – corresponding to a maximum number of taus in the final state – is used to set limits independent of the choice of generation indices.

In analogy to the procedure described in the previous section, limits from chargino and neutralino searches are set for each point in $\mu - M_2 - \tan\beta - m_0$ parameter space. Fig. 6 shows an example of the limit obtained in the gaugino region at $m_0 = 60 \text{ GeV}/c^2$. Due to the destructive interference of the s - and t -channel contributions to the chargino cross section, the limit set by the chargino search does not reach the kinematic limit at small m_0 . On the other hand, the production cross section for $\chi\chi$ is enhanced at small selectron masses, allowing charginos well beyond the kinematic limit to be excluded in certain regions of parameter space.

Limits on the masses of the lightest chargino and neutralino as a function of $\tan\beta$ are obtained by scanning the parameter space in $\mu - M_2 - m_0$ (Fig. 5). Charginos with masses less than $73 \text{ GeV}/c^2$ and neutralinos with masses less than $23 \text{ GeV}/c^2$ are excluded at 95% confidence level for any choice of generation indices i, j, k , and for neutralino, slepton and sneutrino LSPs.

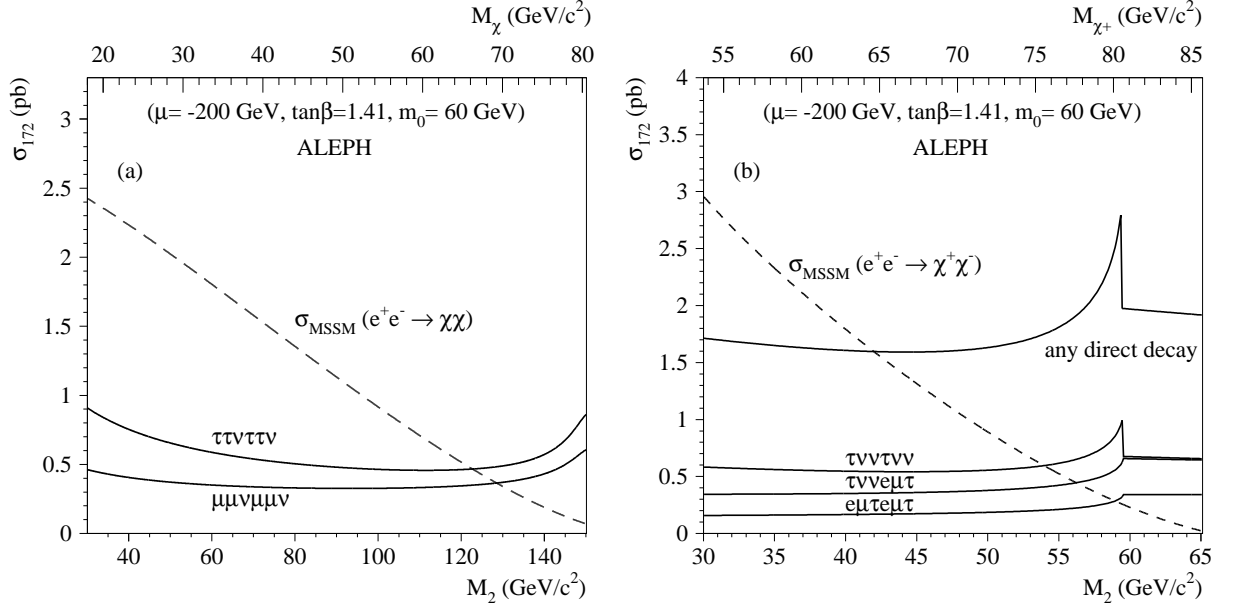


Figure 6: Cross sections at $\sqrt{s} = 172$ GeV excluded at 95% C.L. for pair production of a) the lightest neutralino and b) the lightest chargino, for various final states as a function of M_2 at $\tan\beta = 1.41$, $m_0 = 60$ GeV/ c^2 , $\mu = -200$ GeV/ c^2 . In b) candidates selected at $\sqrt{s} = 161$ GeV are restricted to $m_{\chi^+} < 80.5$ GeV/ c^2 .

7.1.3 Mixed Topologies

For the extreme case of $\Gamma(\chi^+ \rightarrow ff\chi) = \Gamma(\chi^+ \rightarrow fff)$, mixed topologies with one direct and one indirect decay are produced in 50% of the events from chargino pair production. They are selected by the inclusive combination of the “Leptons and Hadrons” and the “Four and Six Leptons plus Missing Energy” analyses, with efficiencies similar to the ones obtained for indirect topologies. As the other half of the events produced consists of direct and indirect topologies, the selection is combined with the corresponding analyses described in the previous sections. The worst case limit is set for $(i, j, k) = (1, 2, 3)$, $(2, 3, 1)$ or $(1, 3, 2)$. In this case all three lepton flavours are accessible in the direct decays, and therefore the combination of all acoplanar lepton selections has to be used, leading to a maximum number of candidates in the data. For the indirect decays, the lightest neutralino can decay into $e\tau\nu$ with a large branching fraction, which corresponds to the smallest efficiency for this generation structure. Therefore this case has been used to set limits independent of the choice for (i, j, k) . This limit is at least as constraining as the limit for direct topologies, the exact position depending on the size of the coupling λ_{ijk} .

7.2 Sleptons

A slepton can decay either directly to a lepton and a neutrino, or indirectly to a lepton and a neutralino, which subsequently decays to two leptons and a neutrino. The decays to charginos are kinematically inaccessible for most of the slepton mass range considered in this section (see previous section). The three types of topologies from the pair-production of sleptons are classified as the *direct topologies* (when both sleptons decay directly), the *indirect topologies* (when both sleptons decay indirectly), and the *mixed topologies* (when one slepton decays directly, one indirectly).

For the *direct topologies* of left-handed sleptons the acoplanar lepton selection was used. Individual efficiencies for the final states ee , $\mu\mu$ and $\tau\tau$ are calculated as a function of the slepton mass, and for the three energies $\sqrt{s} = 133, 161, 172$ GeV. The various final states correspond to different choices of the generation indices i, j, k of the R-parity violating coupling λ_{ijk} . The efficiencies are relatively constant as a function of $M_{\tilde{l}}$, and typical values are given in Table 5. Subtracting the background from Table 4 according to the prescription given in [27], the exclusion cross sections scaled to $\sqrt{s} = 172$ GeV are shown in Fig. 7a for the three final states.

Right-handed sleptons can decay to *two* final states in the direct topology with a 50% branching ratio each for a given choice of the generation indices i, j, k : $\tilde{l}_{kR} \rightarrow \nu_i l_j$ and $\tilde{l}_{kR} \rightarrow \nu_j l_i$. For example, for the coupling λ_{121} pair-produced right-handed selectrons would produce the acoplanar topologies $\frac{1}{4}ee \oplus \frac{1}{2}e\mu \oplus \frac{1}{4}\mu\mu$ with the given branching ratios. The results for admixtures of acoplanar lepton states using the above branching ratios are shown in Fig. 7b. The exclusion cross sections for the right-handed slepton topologies are larger than the exclusion cross sections for their left-handed partners due to the higher background.

For the *indirect topologies*, which consist of six leptons and two neutrinos, an inclusive combination of the “Six Leptons plus \cancel{E} ” and the “Four Leptons plus \cancel{E} ” selection is used, the latter one improving the efficiencies in the region of low and very high neutralino masses. The efficiencies (Table 5) mainly depend on $\Delta M = M_{\tilde{l}} - M_{\chi}$, and are smallest for staus with a λ_{133} coupling at large ΔM . Including the one candidate event observed in the “Four Leptons plus \cancel{E} ” selection (without background subtraction), the 95% C.L. exclusion cross sections scaled to $\sqrt{s} = 172$ GeV are derived, and are shown in Fig. 7c,d for selectrons and a dominant coupling λ_{122} , and for staus with a coupling λ_{133} . The two cases correspond to final states with a maximum number of electrons or muons (which have the largest selection efficiencies), and a maximum number of taus (with the smallest selection efficiencies), respectively.

Pairs of sleptons can produce up to 50% *mixed topologies* in the extreme case when $\Gamma(\tilde{l} \rightarrow l\nu) = \Gamma(\tilde{l} \rightarrow l\chi)$. The mixed topologies are selected by the “Four Leptons plus \cancel{E} ” selection with similar efficiencies to the indirect topologies (Table 5).

The above results are now interpreted within the MSSM. Limits at the 95% C.L. are derived on the masses of the sleptons in the $(M_{\chi}, M_{\tilde{l}_R})$ plane, assuming that only $\tilde{l}_R \tilde{l}_R$ production contributes. This assumption is conservative because of (a) the smaller

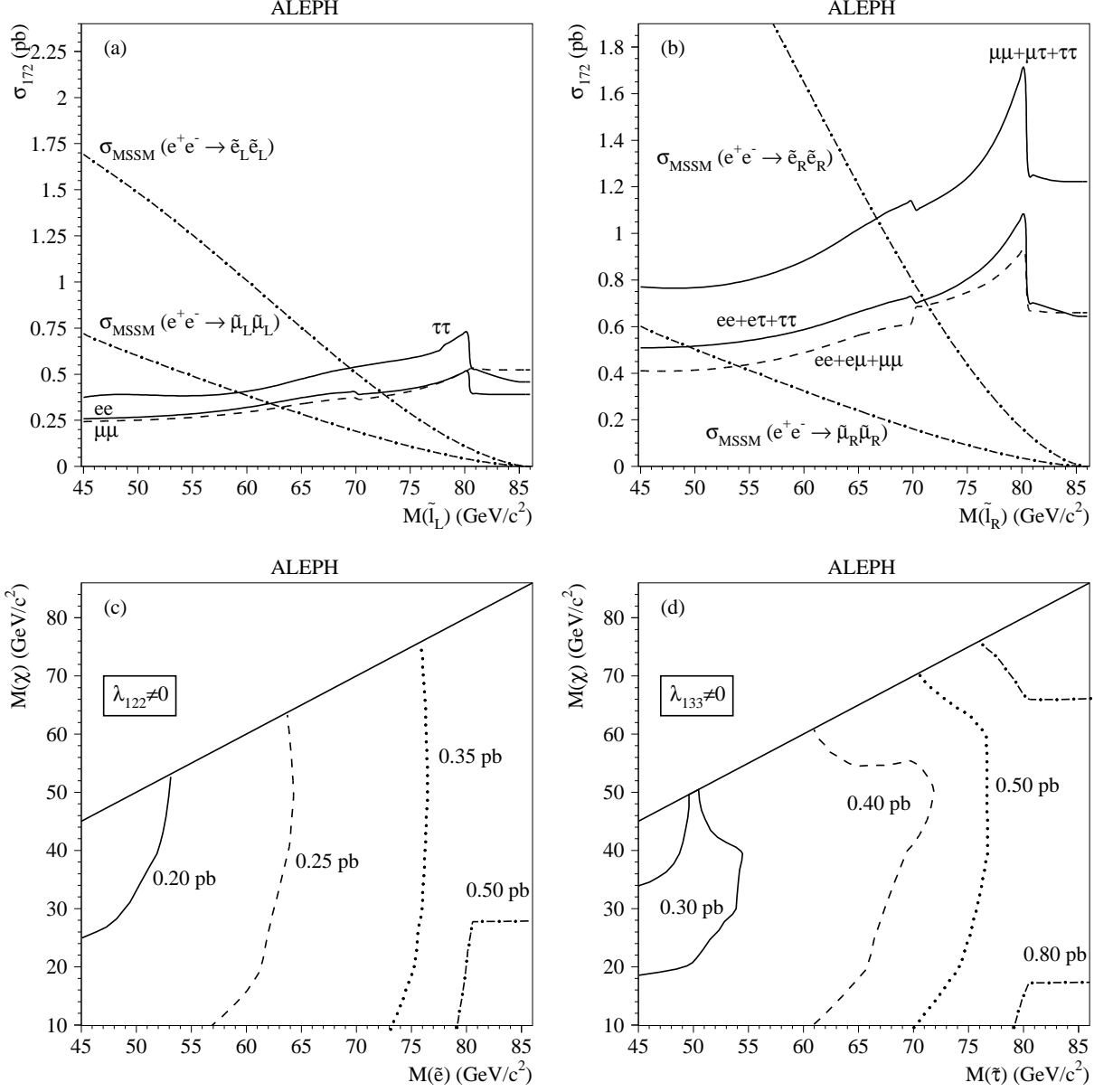


Figure 7: The 95% C.L. slepton exclusion cross sections scaled to $\sqrt{s} = 172$ GeV. For the purpose of these plots a β^3/s cross section dependence, valid for scalar pair-production in the s-channel, was assumed. Fig. a) and b) show $\sigma_{\text{excluded}}^{172}$ for the direct decays of left-handed and right-handed sleptons respectively. Superimposed are the MSSM cross sections at $\tan\beta = 2$ for selectron production ($M_2 = 50$ GeV/c², $\mu = -200$ GeV/c²) and smuon production. Fig. c) and d) show contours of $\sigma_{\text{excluded}}^{172}$ for the indirect decays in the $(M_\chi, M_{\tilde{l}})$ plane for the best-case exclusion ($\tilde{e}\tilde{e}$, λ_{122}) and for the worst-case exclusion ($\tilde{\tau}\tilde{\tau}$, λ_{133}).

Topology	Coupling		
	\tilde{e}_R	$\tilde{\mu}_R$	$\tilde{\tau}_R$
$\frac{1}{4}ee \oplus \frac{1}{2}e\mu \oplus \frac{1}{4}\mu\mu$	λ_{121}	λ_{122}	λ_{123}
$\frac{1}{4}ee \oplus \frac{1}{2}e\tau \oplus \frac{1}{4}\tau\tau$	λ_{131}	λ_{132}	λ_{133}
$\frac{1}{4}\mu\mu \oplus \frac{1}{2}\mu\tau \oplus \frac{1}{4}\tau\tau$	λ_{231}	λ_{232}	λ_{233}

Table 6: *Acoplanar lepton topologies for right-handed sleptons, and their corresponding R-parity violating couplings.*

cross section of right-handed sleptons compared to left-handed sleptons for pure s -channel production, and (b) the larger exclusion cross sections in the direct topologies of right-handed sleptons compared to the left-handed sleptons. The selectron limits are shown in a typical point in the gaugino region ($\mu = -200, \tan\beta = 2$).

Limits are calculated for the two extreme cases of 100% direct or 100% indirect decay modes. This generally corresponds to the two cases when the slepton or the neutralino is the LSP, respectively. If $\Gamma(\tilde{l} \rightarrow l\nu) \sim \Gamma(\tilde{l} \rightarrow l\chi)$, up to 50% *mixed topologies* are also expected for neutralino LSPs in some regions of parameter space. In this case the exclusion region would lie in between the two extreme cases of direct or indirect decays, the exact location of this region depending on the magnitude of the R-parity violating coupling. The limits for the direct and indirect decay modes are shown in Fig. 8. The three choices of couplings for the direct decays correspond to the three possible decay topologies for right-handed sleptons, which are listed in Table 6. In contrast to the limits on the direct smuon and stau topologies, the direct selectron limits show a strong dependence on M_χ owing to the dependence of the cross section on neutralino t -channel interference[29]. Note that the interference is mostly destructive when $M_\chi \gtrsim M_{\tilde{l}_R}$. The two choices $\lambda_{122}, \lambda_{133}$ for the indirect decay modes correspond to the best- and worst-case exclusions, respectively.

For the indirect decay modes, the limits on the sleptons for the most conservative choice of coupling (λ_{133}), and for $M_\chi > 23 \text{ GeV}/c^2$ (the neutralino limit derived in Section 7.1), are: $M_{\tilde{e}_R} > 64 \text{ GeV}/c^2$ (gaugino region, $\mu = -200 \text{ GeV}/c^2, \tan\beta = 2$), $M_{\tilde{\mu}_R} > 62 \text{ GeV}/c^2$, $M_{\tilde{\tau}_R} > 56 \text{ GeV}/c^2$.

7.3 Sneutrinos

A sneutrino can decay either directly to a pair of leptons, or indirectly to a neutrino and a neutralino. The decays to charginos are kinematically inaccessible for most of the sneutrino mass range considered here (see also Section 7.1). The three types of topologies from the pair-production of sneutrinos are again classified as the *direct*, *indirect* and *mixed topologies*.

For the *direct topology* the ‘‘Four Lepton’’ selection is used. The efficiency of pair-produced sneutrinos decaying into the final states $eeee, ee\mu\mu, ee\tau\tau, \mu\mu\mu\mu, \mu\mu\tau\tau, \tau\tau\tau\tau$ are calculated as a function of the sneutrino mass. The different final states correspond

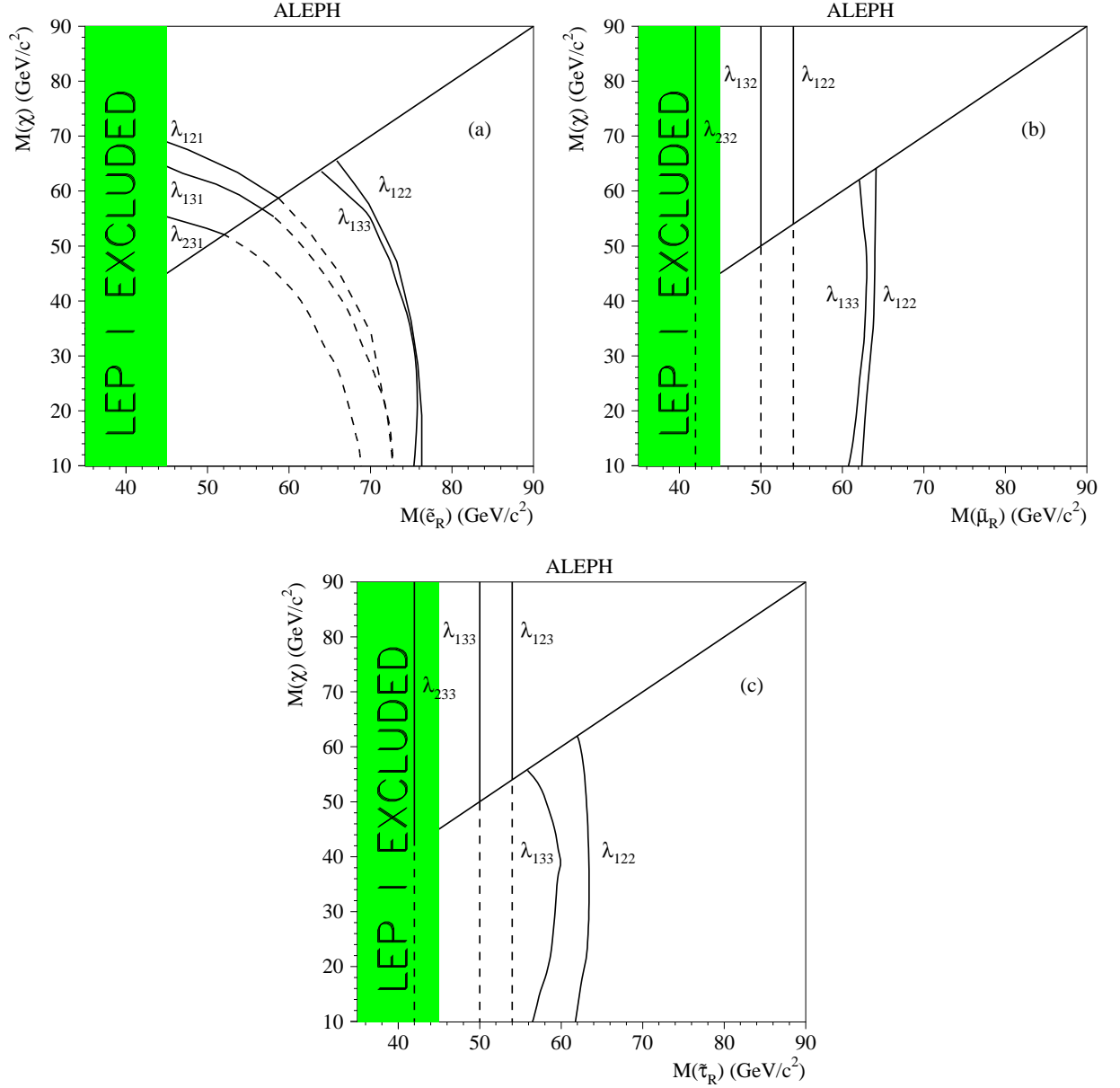


Figure 8: The 95% C.L. limits in the $(m_\chi, m_{\tilde{l}_R})$ plane at $\tan\beta = 2$. Above the diagonal line the lightest neutralino is heavier than the sleptons, and only the direct decays are allowed. Below the line the indirect decays generally dominate, but the branching ratio of the direct (dashed lines) to indirect (full lines) decays depends on the magnitude of the coupling λ_{ijk} . The two choices of λ_{122} and λ_{133} correspond to the best and worst case exclusions for the indirect decays, respectively. Fig. a) shows the selectron limit in the gaugino region for $\mu = -200 \text{ GeV}/c^2$. Fig. b) and c) show the mass limits on smuons and staus.

to different choices of the generation indices i, j, k . The exclusion cross sections scaled to $\sqrt{s} = 172 \text{ GeV}$ are derived combining the data samples from the various energies, and the result is shown in Fig. 9a. Note that sneutrinos have *only one* direct decay mode for a given choice of the generation indices i, j, k .

For the *indirect topologies*, which consist of four leptons and four neutrinos, an inclusive combination of the “Four Leptons plus \cancel{E} ” and the “Four Lepton” selection is used, the latter one increasing the selection efficiencies in the region of small $\Delta M = M_{\tilde{\nu}} - M_{\chi}$. The efficiencies for the sneutrino signal (c.f. Table 5) primarily depend on the neutralino mass, and the lowest efficiencies are found for small M_{χ} . The 95% C.L. exclusion cross sections scaled to $\sqrt{s} = 172 \text{ GeV}$ are shown in Fig. 9b,c for the best- and worst-case couplings λ_{122} and λ_{133} .

As in the slepton case, pairs of sneutrinos can produce up to 50% *mixed topologies*. The efficiencies for the mixed topologies, which are efficiently selected by the “Six Leptons plus \cancel{E} ” selection in combination with the “Four Leptons plus \cancel{E} ” and the “Four Lepton” selections, are generally higher than the efficiencies for indirect topologies, especially for low neutralino masses.

Interpreting these results within the MSSM, the 95% C.L. exclusion regions are derived in the $(M_{\chi}, M_{\tilde{\nu}})$ plane, and are shown in Fig. 10. Exclusions for the two extreme cases of 100% direct or 100% indirect decay modes (which generally correspond to the two cases of sneutrino and neutralino LSPs, respectively) are shown, while the exclusion regions for the case when $\Gamma(\tilde{\nu} \rightarrow l^+l^-) \sim \Gamma(\tilde{\nu} \rightarrow \nu\chi)$ (resulting in a substantial fraction of mixed topologies) would lie in between those two extreme cases. The two choices of couplings for the direct and the indirect topologies correspond to final states with a maximum number of muons or taus, resulting in best- and worst-case exclusion limits, respectively.

For electron-sneutrinos, t -channel chargino exchange can enhance the cross section[30], and this effect is shown by considering a typical point in the gaugino region ($\mu = -200, \tan\beta = 2$) and in the higgsino region ($M_2 = 400 \text{ GeV}/c^2, \tan\beta = 2, \mu < 0$), assuming $\text{BR}(\tilde{\nu} \rightarrow \nu\chi) = 100\%$. For $M_{\chi} < 20\text{-}40 \text{ GeV}/c^2$, sneutrinos can cascade to the chargino, indicated by the dotted lines in Fig. 10a and b, which conservatively assume zero efficiencies for the cascade decays. However, the cascade regions are already excluded by the chargino and neutralino limits of Section 7.1, and are therefore not considered further. The sneutrino mass limits for the indirect decay modes, the most conservative choice of coupling (λ_{133}), and for $M_{\chi} > 23 \text{ GeV}/c^2$ are: $M_{\tilde{\nu}_e} > 72 \text{ GeV}/c^2$ (gaugino region, $\mu = -200 \text{ GeV}/c^2, \tan\beta = 2$), $M_{\tilde{\nu}_e} > 58 \text{ GeV}/c^2$ (higgsino region, $M_2 = 400 \text{ GeV}/c^2, \tan\beta = 2, \mu < 0$), $M_{\tilde{\nu}_\mu}, M_{\tilde{\nu}_\tau} > 49 \text{ GeV}/c^2$.

7.4 Squarks

The stop and sbottom cannot decay *directly* via the purely leptonic $LL\bar{E}$ couplings, but they can decay *indirectly* to the lightest neutralino, producing topologies with four leptons and two jets plus a small amount of missing energy. Using the “Leptons and Hadrons”

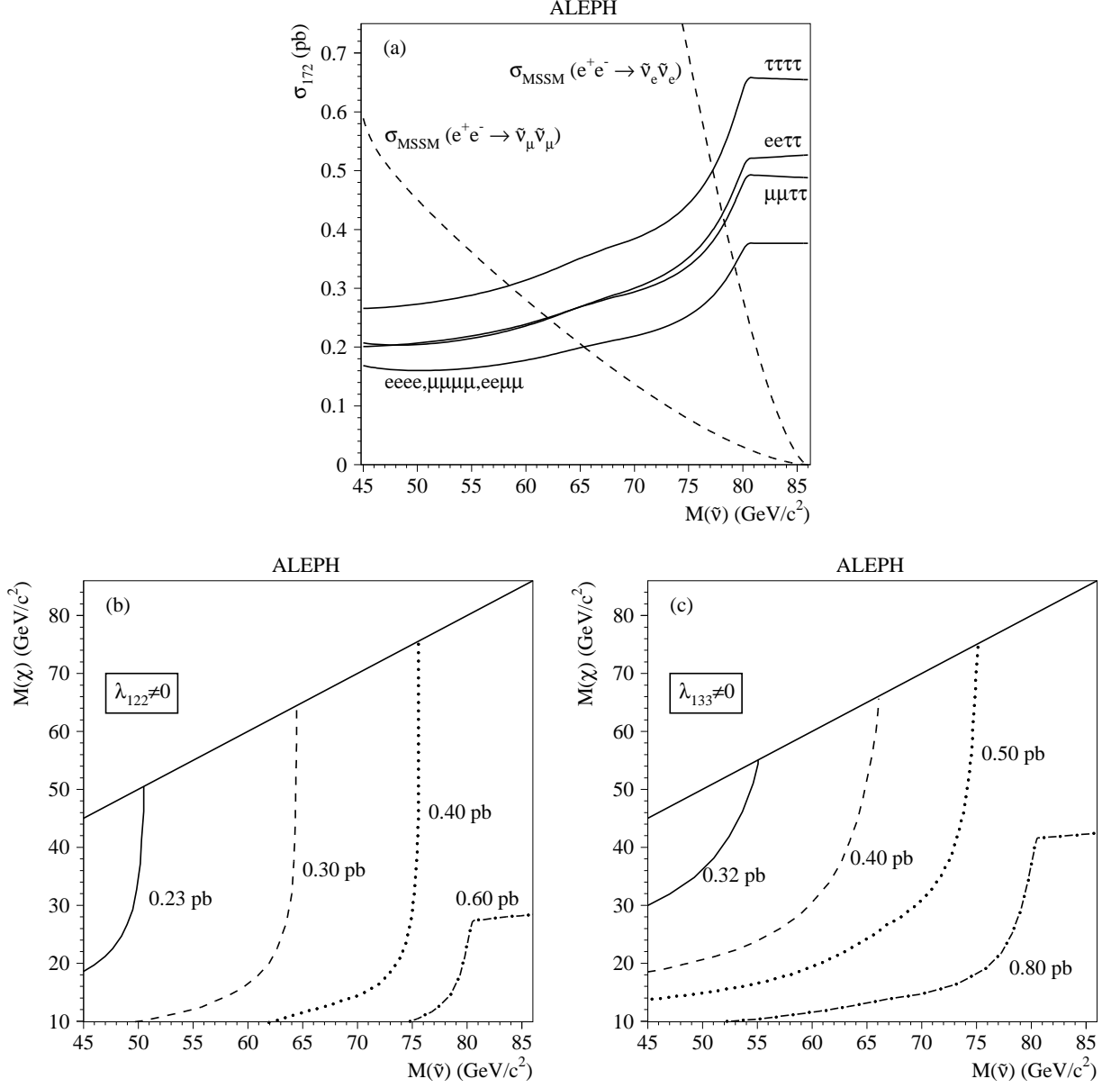


Figure 9: The 95% C.L. sneutrino exclusion cross sections scaled to $\sqrt{s} = 172$ GeV. For the purpose of these plots a β^3/s cross section dependence, valid for scalar pair-production in the s-channel, was assumed. Fig. a) shows $\sigma_{\text{excluded}}^{172}$ for the direct decays of sneutrinos. Superimposed are the MSSM cross sections at $\tan\beta = 2$ for electron-sneutrino production ($M_2 = 100$ GeV/c², $\mu = -200$ GeV/c²) and muon-sneutrino production. Fig. b) and c) show contours of $\sigma_{\text{excluded}}^{172}$ for the indirect decays in the $(M_\chi, M_{\tilde{\nu}})$ plane for the best-case exclusion (λ_{122}) and the worst-case exclusion (λ_{133}).

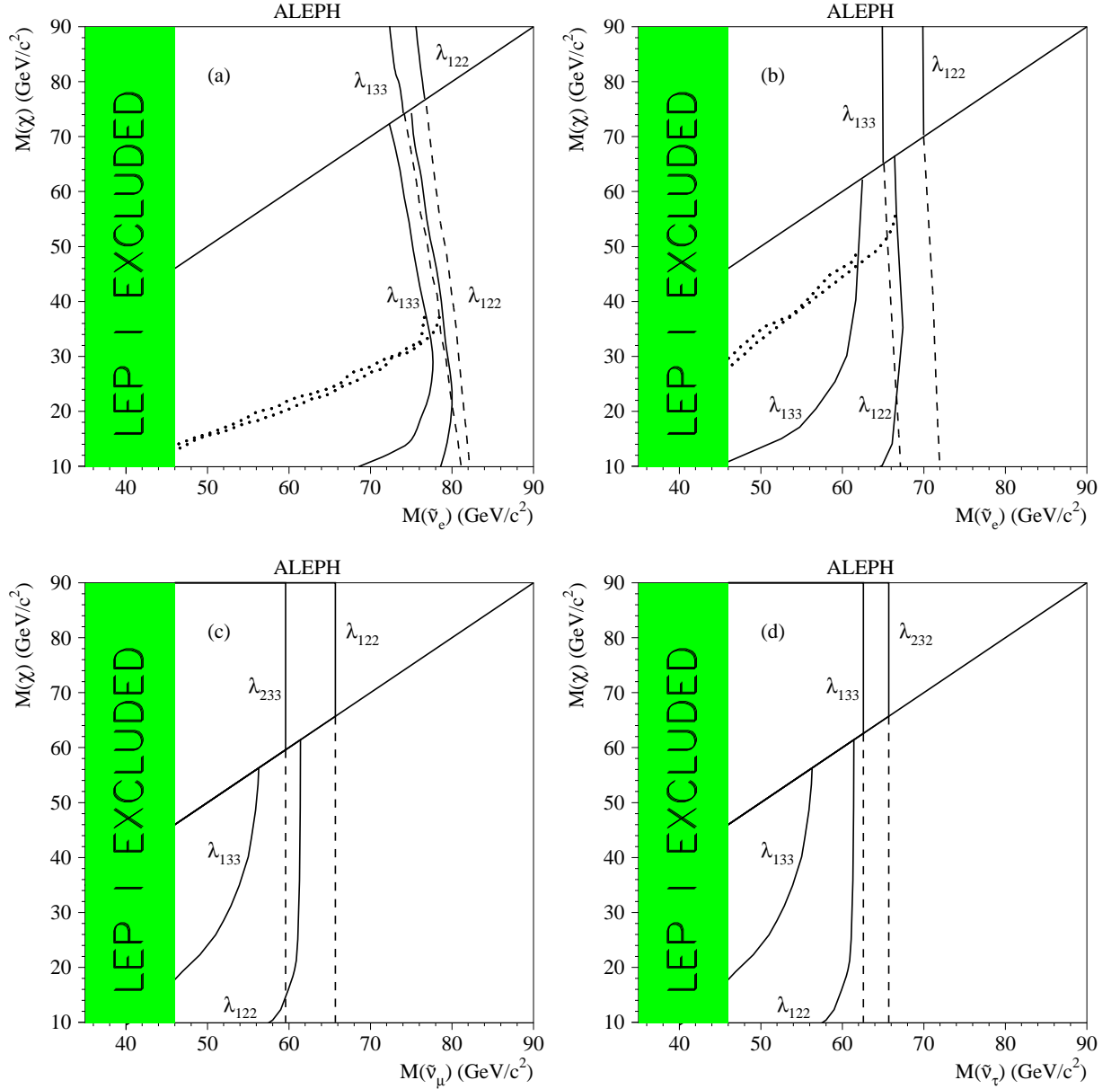


Figure 10: The 95% C.L. limits in the $(m_\chi, m_{\tilde{\nu}})$ plane at $\tan\beta = 2$. Above the diagonal line the lightest neutralino is heavier than the sneutrinos, and only the direct decays are allowed. Below the line the indirect decays generally dominate, but the branching ratio of the direct (dashed lines) to indirect (full lines) decays depends on the magnitude of the coupling λ_{ijk} . The two choices of λ_{122} and λ_{133} correspond to the best and worst case exclusions for the indirect decays. Fig. a) and b) show the electron-sneutrino limit in the gaugino region ($\mu = -200 \text{ GeV}/c$) and the higgsino region ($M_2 = 400 \text{ GeV}/c^2$), respectively, assuming $BR(\tilde{\nu}_e \rightarrow \nu_e \chi) = 100\%$ for the indirect decays (full lines), and conservatively assuming zero efficiency for the cascade decays (dotted lines). Fig. c) and d) show the mass limits on muon- and tau-sneutrinos.

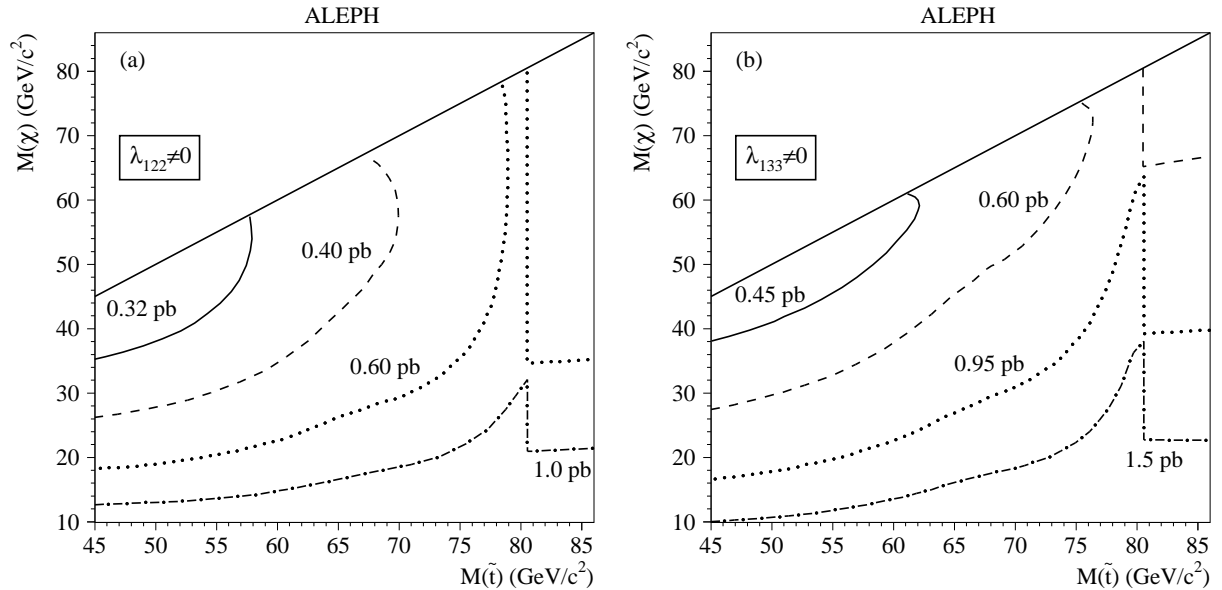


Figure 11: The 95% C.L. stop exclusion cross sections at $\sqrt{s} = 172$ GeV. Fig. a) and b) show contours of $\sigma_{\text{excluded}}^{172}$ in the $(M_\chi, M_{\tilde{t}})$ plane for the best-case exclusion (λ_{122}) and the worst-case exclusion (λ_{133}).

selection, efficiencies (c.f. Table 5) for the stop and sbottom signal are calculated as a function of the squark and neutralino masses and for the three energies. Conservatively, sbottoms have been assumed to hadronise before their decay throughout parameter space, as selection efficiencies for this case are smaller compared to hadronisation after the decay. The excluded cross sections are shown in Fig. 11 for the two couplings λ_{122} and λ_{133} .

The limits in the $(M_\chi, M_{\tilde{q}})$ plane obtained within the MSSM are shown in Fig. 12 for the two choices of couplings λ_{122} , λ_{133} , corresponding to the best- and worst-case exclusions, respectively. For stops, the results for the two mixing angles $\phi_{mix} = 0^\circ, 56^\circ$ correspond to a maximal and minimal \tilde{t}_1 -Z coupling. The limits for the most conservative coupling (λ_{133}) and $M_\chi > 23$ GeV/ c^2 are: $M_{\tilde{t}_L} > 60$ GeV/ c^2 and $M_{\tilde{b}_L} > 58$ GeV/ c^2 ($\phi_{mix} = 0^\circ$), and $M_{\tilde{t}_1} > 44$ GeV/ c^2 ($\phi_{mix} = 56^\circ$).

8 Conclusions

A number of search analyses have been developed to select R-parity violating SUSY topologies from the pair-production of sparticles. It was assumed that the LSP has a negligible lifetime, and that only the $LL\bar{E}$ couplings are non-zero. Limits were derived under the assumption that only one coupling λ_{ijk} is non-zero, although the search analyses cover topologies which would be produced by the simultaneous presence of more than one

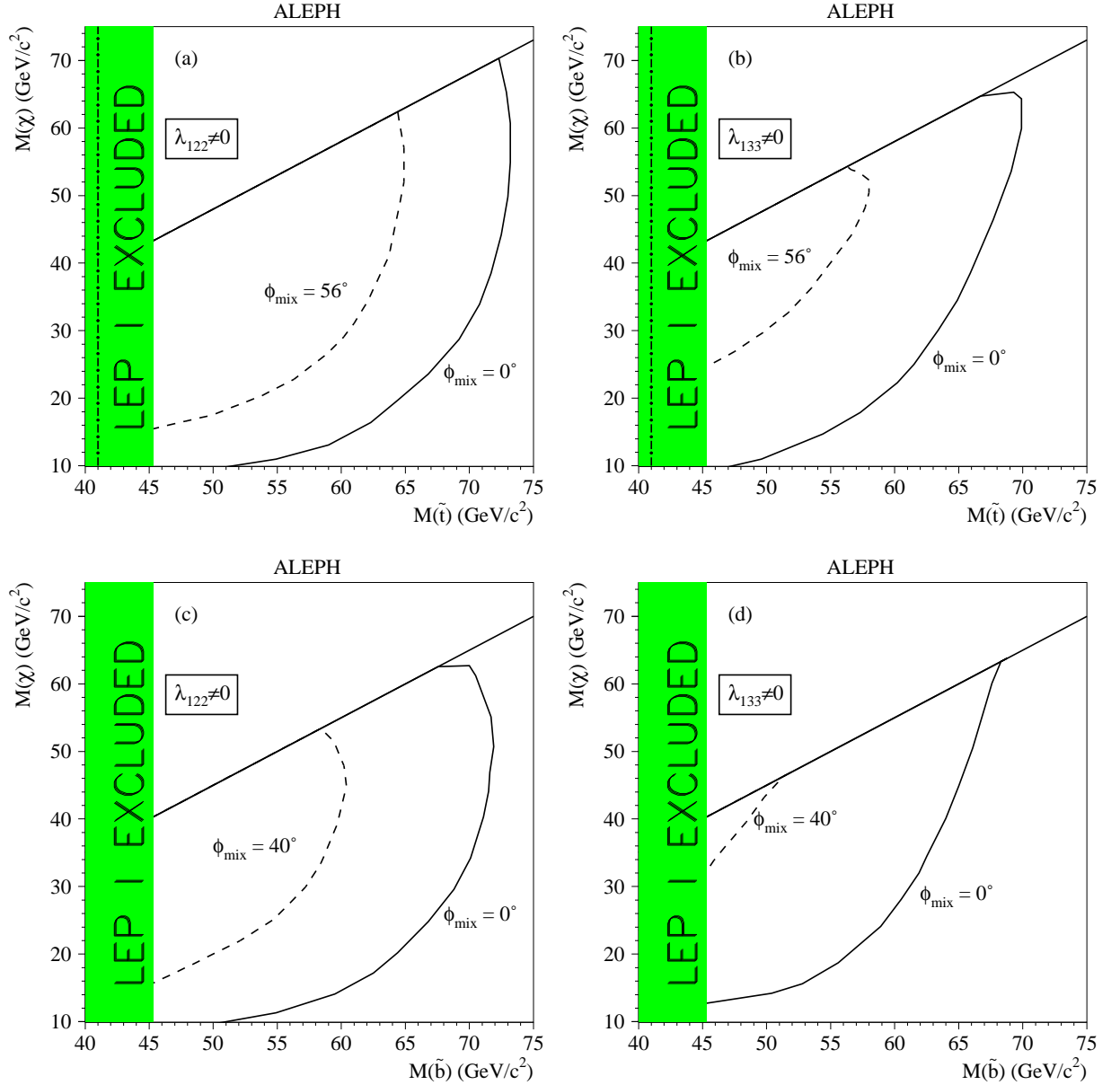


Figure 12: *The 95% C.L. limits on the stop and sbottom in the $(m_\chi, m_{\bar{q}})$ plane. The two choices of λ_{122} and λ_{133} correspond to the best and worst case exclusions, respectively. The mass limits are shown for minimal squark mixing ($\phi_{\text{mix}} = 0^\circ$), and for $\phi_{\text{mix}} = 56^\circ, 40^\circ$ for stops and sbottoms, respectively. The LEP 1 limit for $\phi_{\text{mix}} = 0^\circ$ (and $\phi_{\text{mix}} = 56^\circ$ for stops – dashed-dotted lines) is also shown.*

coupling. Particular emphasis was placed on making no assumption on the nature of the LSP. The search analyses for the various topologies find no evidence for R-parity violating Supersymmetry in the data collected at $\sqrt{s} = 130\text{--}172$ GeV, and limits have been set within the framework of the MSSM.

The decay modes of charginos and heavier neutralinos were classified according to topology into *indirect decay modes* to the lightest neutralino (which generally corresponds to neutralino LSPs), and into *direct decay modes* to three leptons (which generally corresponds to slepton or sneutrino LSPs). At low values of $\tan\beta$, charginos are excluded up to $M_{\chi^+} > 85$ GeV/ c^2 for the indirect decays, and up to $M_{\chi^+} > 80$ GeV/ c^2 for the direct decays. For large $\tan\beta$, the chargino limit drops to $M_{\chi^+} > 78$ GeV/ c^2 and $M_{\chi^+} > 73$ GeV/ c^2 , respectively. The weakest mass bound on the lightest neutralino is found at $\tan\beta = 1$, where $M_{\chi} > 25$ GeV/ c^2 for the indirect (chargino) decays, and $M_{\chi} > 23$ GeV/ c^2 for the direct decays. The mass bound is much stronger at large values of $\tan\beta$, where $M_{\chi} > 47$ GeV/ c^2 and $M_{\chi} > 45$ GeV/ c^2 for the two chargino decay modes at $\tan\beta > 15$. The limits for charginos and neutralinos hold for any choice of the generation indices i, j, k of the coupling λ_{ijk} , and neutralino, slepton and sneutrino LSPs.

The mass limits for the sfermions are highly dependent on the choice of the indices i, j, k and the nature of the LSP, mainly owing to the much smaller production cross section of scalars compared to the fermionic cross sections. For the indirect decay modes (where the sfermions decay to the lightest neutralino) and the most conservative choice of coupling, the mass limits at $\tan\beta = 2$ are:

- $M_{\tilde{e}_R} > 64$ GeV/ c^2 (gaugino region),
- $M_{\tilde{\mu}_R} > 62$ GeV/ c^2 ,
- $M_{\tilde{\tau}_R} > 56$ GeV/ c^2 ,
- $M_{\tilde{\nu}_e} > 72$ GeV/ c^2 (gaugino region),
- $M_{\tilde{\nu}_\mu}, M_{\tilde{\nu}_\tau} > 49$ GeV/ c^2 ,
- $M_{\tilde{t}_L} > 60$ GeV/ c^2 ,
- $M_{\tilde{b}_L} > 58$ GeV/ c^2 .

These mass limits considerably improve upon existing limits.

9 Acknowledgements

It is a pleasure to congratulate our colleagues from the accelerator divisions for the successful operation of LEP at high energy. We would like to express our gratitude to the engineers and support people at our home institutes without whose dedicated help this work would not have been possible. Those of us from non-member states wish to thank CERN for its hospitality and support.

References

- [1] For a review see for example H.P. Nilles, Phys. Rep. **110** (1984) 1; H. E. Haber and G. L. Kane, Phys. Rep. **117** (1985) 75.
- [2] S. Weinberg, Phys. Rev. **D 26** (1982) 287; N. Sakai and T. Yanagida Nucl. Phys. **B 197** (1982) 83; S. Dimopoulos, S. Raby and F. Wilczek, Phys. Lett. **B 212** (1982) 133.
- [3] G. Farrar and P. Fayet, Phys. Lett. **B 76** (1978) 575.
- [4] L. J. Hall and M. Suzuki, Nucl. Phys. **B 231** (1984) 419; D. E. Brahm, L. J. Hall, Phys. Rev. **D 40** (1989) 2449; L. E. Ibanez, G. G. Ross, Nucl. Phys. **B 368** (1992) 3; A. Chamseddine and H. Dreiner, Nucl. Phys. **B 458** (1996) 65; A. Yu. Smirnov, F. Vissani, Nucl. Phys. **B 460** (1996) 37.
- [5] S. Dimopoulos, L.J. Hall, Phys. Lett. **B 207** (1988) 210; V. Barger, G. F. Giudice and T. Han, Phys. Rev. **D40** (1989) 2987
- [6] H. Dreiner, S. Lola, “*R-parity Violation*”, in the proceedings of the Workshop *Physics at LEP 2*, eds. G. Altarelli, T. Sjöstrand, and F. Zwirner, CERN 96-01 and hep-ph/9602207; J. Erler, J. L. Feng and N. Polonsky, Phys. Rev. Lett. **78** (1997) 3063; J. Kalinowski, R. Ruckl, H. Spiesberger, P. M. Zerwas, Phys. Lett. **B 406** (1997) 314-320; L3 Collaboration, “*Search for R-parity Breaking Sneutrino Exchange at LEP*”, CERN-PPE/97-99 (1997), submitted to Phys. Lett. **B**.
- [7] B. C. Allanach, H. Dreiner, P. Morawitz and M. D. Williams, “*Single Sneutrino/Slepton Production at LEP2 and the NLC*”, hep-ph/9708495, submitted to Phys. Lett. **B**.
- [8] ALEPH Collaboration, Phys. Lett. **B 349** (1995) 238.
- [9] ALEPH Collaboration, Phys. Lett. **B 384** (1996) 461.
- [10] J. Ellis, et al., Nucl. Phys. **B 238** (1984) 453.
- [11] H. Dreiner and P. Morawitz, Nucl. Phys. **B 428** (94) 31; H. Dreiner, S. Lola, P. Morawitz, Phys. Lett. **B 389** (1996) 62.
- [12] D. P. Roy, Phys. Lett. **B 283** (1992) 270.
- [13] H. Dreiner, “*An Introduction to Explicit R-parity Violation*”, hep-ph/9707435, to be published in “*Perspectives on Supersymmetry*”, edited by G.L. Kane, World Scientific.
- [14] S. Dawson, Nucl. Phys. **B 261** (1985) 297.
- [15] ALEPH Collaboration, Nucl. Instr. Meth. **A 294** (1990) 121.
- [16] ALEPH Collaboration, Nucl. Instr. Meth. **A 360** (1995) 481.

- [17] S. Katsanevas, P. Morawitz, “*SUSYGEN 2.2 - A Monte Carlo Event Generator for MSSM Sparticle Production at e^+e^- Colliders*”, hep-ph/9711417, submitted to Comp. Phys. Comm.
- [18] ALEPH Collaboration, “*Searches for Scalar Top and Scalar Bottom Quarks at LEP2*”, CERN-PPE/97-084 (1997), submitted to Phys. Lett. **B**.
- [19] T. Sjöstrand, “*The PYTHIA 5.7 and JETSET 7.4 Manual*”, LU-TP 95/20, CERN-TH 7112/93, Comp. Phys. Comm. **82** (1994) 74.
- [20] M. Skrzypek, S. Jadach, W. Placzek and Z. Was, Comp. Phys. Comm. **94** (1996) 216.
- [21] H. Anlauf et al., Comp. Phys. Comm. **79** (1994) 466.
- [22] S. Jadach and Z. Was, Comp. Phys. Comm. **36** (1985) 191.
- [23] J.A.M. Vermaseren in “*Proceedings of the IVth international Workshop on Gamma Gamma Interactions*”, Eds. G. Cochard and P. Kessler, Springer Verlag, 1980.
- [24] J. -F. Grivaz and F. Le Diberder, “*Complementary analyses and acceptance optimization in new particle searches*”, LAL preprint # 92-37 (1992).
- [25] ALEPH Collaboration, Phys. Lett. **B 373** (1996) 246.
- [26] ALEPH Collaboration, “*Search for sleptons in e^+e^- collisions at centre-of-mass energies of 161 GeV and 172 GeV*”, CERN-PPE/97-056 (1997), submitted to Phys. Lett. B.
- [27] R. M. Barnett et al., Phys. Rev. **D 54** (1996) 1.
- [28] K. Inoue, A. Kakuto, H. Komatsu, and S. Takeshita, Prog. Theor. Phys. **68** (1982) 927; *ibid.* **71** (1984) 413.
- [29] A. Bartl, H. Fraas, W. Majerotto, Z. Phys. **C 34** (1987) 411.
- [30] V. Barger, W.-Y. Keung, R.J.N. Phillips, Phys. Lett. **B 364** (1995) 27.